



# The potential contributions of phytoplankton cells and zooplankton fecal pellets to POC export fluxes during a spring bloom in the East China Sea



Yong Qiu<sup>a</sup>, Edward A. Laws<sup>b</sup>, Lei Wang<sup>c</sup>, Dazhi Wang<sup>a</sup>, Xin Liu<sup>a,\*</sup>, Bangqin Huang<sup>a</sup>

<sup>a</sup> Fujian Provincial Key Laboratory of Coastal Ecology and Environmental Studies, State Key Laboratory of Marine Environmental Science, College of the Environment and Ecology, Xiamen University, Xiamen 361102, China

<sup>b</sup> Department of Environmental Sciences, College of the Coast and Environment, Louisiana State University, Baton Rouge, Louisiana, USA

<sup>c</sup> Third Institute of Oceanography, State Oceanic Administration, Xiamen 361005, China

## ARTICLE INFO

### Keywords:

Phytoplankton  
Bloom  
Sinking rate  
Fecal pellet  
POC flux  
East China Sea

## ABSTRACT

Sinking particles are mainly composed of phytoplankton cells and zooplankton fecal pellets, but the proportions of these sources contribute to the overall particulate organic carbon (POC) flux are highly variable temporally and spatially. Here, we report for the first time simultaneous estimates of the POC fluxes from phytoplankton cells and zooplankton fecal pellets during a spring bloom in the East China Sea. The sinking rate of phytoplankton during the bloom event was  $12 \pm 2 \text{ m d}^{-1}$ , which was more than 10 times the rate at non-bloom stations ( $1.0 \pm 0.8 \text{ m d}^{-1}$ ). Microscopic observations indicated that the formation of aggregates by the *Prorocentrum donghaiense* (the dominant phytoplankton species) enhanced the sinking rates during the bloom. These enhanced sinking rates and 10 times higher phytoplankton biomass during the bloom increased POC fluxes to as high as  $24 \text{ g C m}^{-2} \text{ d}^{-1}$ , about 100 times the rate at reference non-bloom stations ( $0.26 \text{ g C m}^{-2} \text{ d}^{-1}$ ). The POC flux of fecal pellets at bloom stations ( $0.95\text{--}1.4 \text{ g C m}^{-2} \text{ d}^{-1}$ ) increased to only about 6 times the rates at non-bloom stations ( $0.20\text{--}0.25 \text{ g C m}^{-2} \text{ d}^{-1}$ ). The fecal pellet POC flux was mainly enhanced by the increase of phytoplankton abundance, which led to higher mesozooplankton grazing rates and fecal pellet production rates during the bloom. In summary, the majority of the enhanced sinking POC flux during the bloom was directly associated with phytoplankton sinking. This enhanced flux sequestered carbon faster than anticipated because of the enhancements of both phytoplankton sinking rates and abundance. Such dramatic, albeit brief, events make very important potential contributions to the annual POC flux.

## 1. Introduction

The global ocean is the largest carbon reservoir on Earth's surface and plays a dominant role in the global carbon cycle (Le Quéré et al., 2015). About 50 Gt of carbon are fixed via photosynthesis by phytoplankton communities in the euphotic zone of the ocean every year (Bach et al., 2016). However, the global ocean CO<sub>2</sub> sink is only about  $2.6 \pm 0.5 \text{ Gt C yr}^{-1}$ , about 5% of the photosynthetically fixed carbon (Le Quéré et al., 2016). The biological pump, which is the principal mechanism responsible for transporting organic carbon from ocean surface waters to the deep sea, is generally considered to be inefficient because the flux of organic carbon to the deep sea is only about 1–3% of the rate of primary production in the euphotic zone (Neuer et al., 2002). Most of the particulate organic carbon (POC) is lost during the sinking process via a complex suite of biogeochemical processes (Honjo et al., 2014). High POC concentrations in surface waters and rapid

sinking therefore would enhance export production from surface waters to the seabed.

Sinking POC is composed mainly of phytoplankton cells, zooplankton fecal pellets, organic aggregates, and dead plankton (Turner, 2002). Overall, phytoplankton make the largest contribution to the POC pool in the upper ocean, a significantly higher contribution than that of zooplankton fecal pellets and other particles. However most laboratory studies have indicated that the sinking rates of phytoplankton cells are typically  $< 1\text{--}10 \text{ m d}^{-1}$ , significantly lower than the sinking rates of other major particles (Smetacek et al., 1978; Bienfang, 1980, 1981; Pakhomov et al., 2002). Therefore, many studies of POC fluxes have usually ignored direct sinking of phytoplankton cells, and in particular of picophytoplankton (Turner, 2002). Nevertheless, recent research has indicated that phytoplankton can be transported to the sea bottom within large, rapidly sinking aggregations of zooplankton fecal pellets, phytoplankton cells, and diverse assemblages of particulate organic

\* Corresponding author.

E-mail address: [liuxin1983@xmu.edu.cn](mailto:liuxin1983@xmu.edu.cn) (X. Liu).

<https://doi.org/10.1016/j.csr.2018.08.001>

Received 10 March 2018; Received in revised form 24 July 2018; Accepted 2 August 2018

Available online 08 August 2018

0278-4343/ © 2018 Elsevier Ltd. All rights reserved.

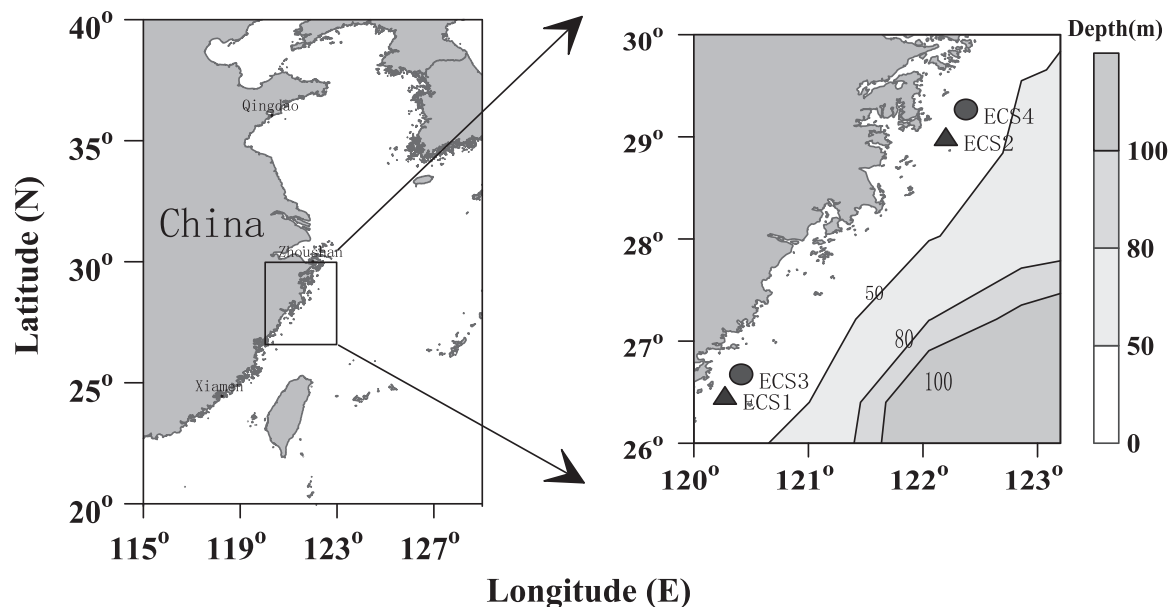


Fig. 1. Study stations in the coastal of the East China Sea. Stations ECS1 and ECS2 were bloom stations (show in triangles), while ECS3 and ECS4 were reference stations (show in circles).

matter (Waite et al., 2000; Steinberg and Landry, 2017). In brief, sinking of POC involves two main pathways. The first is the sinking of fecal pellets excreted by herbivorous zooplankton; the second is the direct sinking of individual phytoplankton cells (e.g., diatoms and coccolithophorids) or aggregations of phytoplankton cells and other particles that stick together under certain circumstances and thereby form larger particles that are exported into the deep sea (Turner, 2015).

The contributions of phytoplankton and zooplankton fecal pellets to the overall POC flux vary greatly over a range of temporal and spatial scales (Butler and Dam, 1994; Gutiérrez-Rodríguez et al., 2010). A review by Turner (2002) of the contribution of zooplankton fecal pellets to the total POC flux has revealed that it ranges from nearly 0–99% in different plankton communities around the world. In the Gulf of St. Lawrence, the flux of POC in fecal pellets represents 3–100% of the total POC flux (Roy et al., 2000). In the Scotia Sea, Antarctica, the analogous proportions range from 42% to 59% (Belcher et al., 2016). Generally, fecal pellets account for at most 60% of the total POC flux in shelf areas (Smith et al., 2002). In the open ocean, the contribution of fecal pellets to the total POC flux ranges from 14% to 35% at ALOHA station (Wilson et al., 2008). These data suggest that sinking fecal pellets may account for the majority of the POC fluxes in marginal seas and nearshore areas, where the high concentrations of phytoplankton are a rich source of food for herbivorous zooplankton. However, many reports have indicated that sinking of phytoplankton cells plays an important and unique role in the POC flux in coastal areas, especially during algal blooms (Gutiérrez-Rodríguez et al., 2010; Ebersbach et al., 2014).

During blooms, particles often form aggregates that greatly increase the sinking rates of phytoplankton cells. This mechanism has been invoked to explain the mass sedimentation of phytoplankton blooms in the ocean (Kiørboe and Hansen, 1993; Durkin et al., 2016). The size of the aggregates can be as much as several millimeters to several centimeters (Seebah et al., 2014), and their sinking rates can range from tens to hundreds of meters per day (Turner, 2015). However, zooplankton grazing and egestion rates can increase more than ten times during a bloom (Gleiber et al., 2015). Therefore, both phytoplankton cells and zooplankton fecal pellets are important components of sinking POC in coastal areas (Turner, 2002).

Marginal seas play an important role in the global oceanic carbon cycle. They account for only about 10% of the surface area of the global ocean but contribute approximately 28% of global primary production

and about 80% of organic carbon burial (Sabine and Hood, 2003). The East China Sea (ECS) is one of the largest marginal seas in the Western Pacific and has a high primary production rate of  $0.3\text{--}1.5\text{ g C m}^{-2}\text{ d}^{-1}$  (Gong et al., 2003). POC fluxes have been determined by various approaches in the ECS (Hung et al., 1999, 2009; Hoshika et al., 2003; Oguri et al., 2003; Iseki et al., 2003; Guo and Zhang, 2005; Zhu et al., 2006; Hung and Gong, 2011). Model-estimated organic carbon burial on the broad ECS shelf is  $7\text{--}10\text{ Mt C yr}^{-1}$  (Chen and Wang, 1999), and the estimated rate of organic carbon offshore transport is  $2\text{--}12\text{ Mt C yr}^{-1}$  (Liu et al., 2006). Several studies have deployed sediment traps to measure POC fluxes in the ECS (Iseki et al., 2003; Guo et al., 2010; Hung et al., 2013). Iseki et al. (2003) have shown that POC fluxes measured by moored sediment traps were  $300\text{--}5000\text{ mg C m}^{-2}\text{ d}^{-1}$  over the continental shelf and Okinawa Trough in the ECS (Iseki et al., 2003). Hung et al. (2013) have reported that POC fluxes estimated directly from sediment traps were  $720\text{--}7300\text{ mg C m}^{-2}\text{ d}^{-1}$  in the ECS. After using a vertical mixing model to correct the fluxes for bottom resuspension, they estimated the POC fluxes on the inner shelf of the ECS to be  $486\text{--}785\text{ mg C m}^{-2}\text{ d}^{-1}$ .

Spring phytoplankton blooms have been recurrent events in the ECS during recent years, with *Prorocentrum donghaiense* the dominant species from late April to May (Tang et al., 2006; Guo et al., 2014). Guo et al. (2016) measured phytoplankton sinking rates of  $0.13\text{--}1.04\text{ m day}^{-1}$  using the SETCOL method (Bienfang, 1981) during a bloom in the ECS. Phytoplankton blooms can lead to substantial carbon export via sinking of phytoplankton cells in bloom areas (Turner, 2002). The relative contributions of phytoplankton and zooplankton fecal pellets to the total POC sinking flux during such spring blooms are unknown. No previous study has involved simultaneous estimation of the contributions of sinking fecal pellets and phytoplankton cells to the total flux of sinking POC during a spring bloom in a marginal sea. In this study, we simultaneously estimated the POC contents and fluxes of both phytoplankton cells and zooplankton fecal pellets in the coast waters of the ECS. Our goals were to compare these two main contributors to the total POC flux in the bloom and non-bloom areas and to elucidate the underlying mechanisms responsible for the variations of POC export in marginal seas.

## 2. Materials and methods

### 2.1. Study area and sampling methods

We studied a phytoplankton bloom that occurred in the coastal waters of the ECS during 1–6 May 2016. The depths of all the stations in this study were less than 50 m (Fig. 1). Based on chlorophyll *a* (Chl *a*) concentration and cell abundances, we defined stations ECS1 and ECS2 as the bloom stations; stations ECS3 and ECS4 were nearby non-bloom stations used for reference purposes.

All water samples were collected at three water depths (2 m, 15 m, and 35 m) using a Seabird conductivity-temperature-depth (CTD) rosette system (SBE 9/11 plus) equipped with twelve Niskin bottles (12 L). The water samples were analyzed for Chl *a*, phytoplankton abundance, and sinking rates. Seawater samples (100–500 mL, according to concentration) for Chl *a* analysis were filtered onto GF/F filters (0.25 cm, Whatman) under a vacuum pressure less than 75 mm Hg and in dim light and then kept frozen in liquid nitrogen until analysis. Chl *a* concentrations were determined by the acidification method with a Turner Designs fluorometer after extraction in 90% acetone at 4 °C in the dark for 20 h (Strickland and Parsons, 1972). Integral average Chl *a* concentrations were calculated by numerical integration of the concentrations at the three sample depths. Temperature, salinity, and depth were recorded by CTD. Fluorescence Chl *a* and turbidity data were recorded by the fluorescent probe and turbidimeter attached to the CTD, respectively.

### 2.2. Sample analysis methods

Phytoplankton seawater samples were carefully transferred to SETCOL columns (Bienfang, 1981) for measurement of sinking rates. We used a SETCOL length of 0.6 m and a water volume of about 2 L. The phytoplankton cell abundances were measured by counting phytoplankton cells observed at 8× magnification with an optical Zoom-stereo microscope (Rixin-SZM). The column integral average cell abundance was estimated by numerical integration of the abundances at the sampling depths.

We used Eq. (1) to calculate the cell volumes of dinoflagellates. The linear dimensions of the cells were estimated by microscopic examination. Volumes of other phytoplankton were determined using the methodology of Sun and Liu (2003). The linear dimensions of 30 or more individual cells were measured to obtain precise estimates. Then, we estimated the average cell carbon content of the phytoplankton using Eq. (2) from Eppley et al. (1970). The final POC content of the phytoplankton samples was estimated from the product of cell carbon content and cell concentration (Eq. (3)).

$$\text{Cell volume: } V = \frac{\pi}{12} \times a \times b^2 \quad (1)$$

$$\text{Log}_{10} C (\text{pg C cell}^{-1}) = 0.94 \times \text{Log}_{10} V - 0.60 \quad (2)$$

$$\text{PC} (\text{mg C L}^{-1}) = N \times C \times 10^{-6} \quad (3)$$

where *V* is the volume of a *Prorocentrum* cell, *a* is the cell length (transapical section), *b* is the cell width (cross section), *C* is the POC content of a phytoplankton cell, *N* is the concentration of phytoplankton cells (number per liter), and *PC* is the POC concentration associated with phytoplankton.

In this study, the average sinking rate of the phytoplankton population was measured in a settling column by the SETCOL method (Bienfang, 1981; Liu and Wu, 2016). The SETCOL columns were identical to the columns described by Bienfang (1981) and filled with seawater samples. Sinking rates were calculated according to Eq. (4):

$$\psi = N_s/N_t \times \frac{L}{t} \quad (4)$$

where  $\psi$  is the average sinking rate ( $\text{m d}^{-1}$ ); *L* is the height of the

SETCOL column (0.6 m); *t* is the duration of the trial (0.021 d or about 30 min); *N<sub>t</sub>* is the total number of phytoplankton cells in the SETCOL column; and *N<sub>s</sub>* is the total number of phytoplankton cells that settled during the trial time.

We examined three replicate samples of seawater under the microscope to obtain the concentration of phytoplankton cells, which was multiplied by the volume of the column.

Bloom seawater phytoplankton aggregates samples were diluted in different proportions with 0.2- $\mu\text{m}$  capsule filtered seawater from the same aliquot. The number of aggregates counted under the microscopic did not change significantly before dilution. The dilution factors were 1, 2, 4, 8, 16, and 32. Then the sinking rates of the aggregates diluted by the different dilution factors were measured by the SETCOL method to determine how the sinking rates of the phytoplankton aggregates changed with aggregate abundance.

Phytoplankton POC fluxes were estimated as the product of the average of the SETCOL sinking rates and the average phytoplankton POC content integrated through the water column (Shanks and Trent, 1980; Guo et al., 2016):

$$\begin{aligned} F_p &= \text{average } \Psi_p \times \text{Integral average } C_p \\ &= \left[ \frac{\Psi_{Z1} + \Psi_{Z2} + \Psi_{Z3}}{3} \right] \times \frac{[(C_{Z1} + C_{Z2}) \times (Z2 - Z1) / 2 + (C_{Z2} + C_{Z3}) \times (Z3 - Z2) / 2]}{Z3} \end{aligned} \quad (5)$$

where  $F_p$  ( $\text{g C m}^{-2} \text{d}^{-1}$ ) is the POC flux of phytoplankton,  $C_p$  ( $\text{g C m}^{-3}$ ) is the average carbon content of the phytoplankton cells, and  $\Psi_p$  ( $\text{m d}^{-1}$ ) is the phytoplankton sinking rate.  $\Psi_{z_m}$  is the sinking rate of the phytoplankton at depth *Z* meters (*Z*<sub>1</sub>, *Z*<sub>2</sub>, *Z*<sub>3</sub> = 5 m, 15 m, and 35 m, respectively), and the *C<sub>Z</sub>* is the corresponding POC content of phytoplankton at depth *Z* meters.

Zooplankton copepods were collected with a vertical tow from the bottom (35 m, consistent with the maximum depth of the CTD) to the surface using zooplankton nets with mesh sizes of 200  $\mu\text{m}$  and a non-filtering cod end (Svensen et al., 2014). In the shipboard laboratory, zooplankton samples were divided into three body-length groups based on mesh size: a large group (> 1000  $\mu\text{m}$ ), medium group (500–1000  $\mu\text{m}$ ), and a small group (200–500  $\mu\text{m}$ ) (Wang and Fan, 1997; Møller et al., 2010). Fecal pellets were picked from the vertical trawl samples from the bottom (35 m, consistent with the maximum depth of CTD) to the surface with a 60- $\mu\text{m}$  mesh net (Manno et al., 2015). The water was then filtered through 500- $\mu\text{m}$ -mesh netting to remove large zooplankton and other detritus. In accord with the Manno et al. (2015) method, the fecal pellet samples were divided into five kinds of shapes (ovoid, round, cylindrical, tabular, and ellipsoidal). Fecal pellets were randomly collected under a dissecting microscope with a fine-mouthed pipette, and their volumes were estimated with geometric formulae at the same time. The pellets were classified into three groups based on their volumes: a small (200–500  $\times 10^3 \mu\text{m}^3$ ), medium (500–5000  $\times 10^3 \mu\text{m}^3$ ), and large group (> 5000  $\times 10^3 \mu\text{m}^3$ ). We trawled three times at each site, and the number of fecal pellets exceeded 600 per group. These pellets were used to determine the sinking rates and carbon contents of fecal pellets. Fecal pellets were rinsed with filtered (< 0.2  $\mu\text{m}$ ) seawater on a 60- $\mu\text{m}$  sieve before being used to measure sinking rates. The fecal pellets were then carefully mixed into 60-micron filtered seawater in the SETCOL columns. After 5 min, the fecal pellets at the lower end of the SETCOL columns were collected and counted to determine their average sinking rate.

The fecal pellets in each group were filtered onto Whatman GF/F filters after being rinsed three times with Milli-Q water. All the GF/F filters were precombusted combusted at 500 °C for 6 h in muffle burner (Hung et al., 2013). The fecal pellets on the GF/F filters were sealed in a 10-mL polycarbonate column and kept frozen (− 20 °C) prior to determination of their POC content in the lab with an elemental analyzer (Perkin Elmer model 2400 CHN Analyzer). The fecal pellet POC content in the seawater,  $P_{FP}$  ( $\text{g m}^{-3}$ ), was calculated with Eq. (6):

$$F_{FP} = C_{FP} \div (M \times D) \quad (6)$$

where  $C_{FP}$  is the mass of fecal pellet POC in the net cod end (g);  $M$  is the mesh area of the zooplankton net ( $m^2$ ); and  $D$  is the depth of the trawl net (m).

The total fecal pellet POC flux was calculated as the sum of the product of the fecal pellet POC content in each size category and the corresponding average sinking rate for that category (Dagg et al., 2014):

$$F_{FP} = C_S \times \text{average} \Psi_S + C_M \times \text{average} \Psi_M + C_L \times \text{average} \Psi_L \quad (7)$$

where  $F_{FP}$  is the total POC flux of zooplankton fecal pellets ( $g C m^{-2} d^{-1}$ ),  $C_S$ ,  $C_M$ , and  $C_L$  are the POC contents of the small, medium, and large fecal pellets ( $g C m^{-3}$ ), respectively, and  $\Psi_S$ ,  $\Psi_M$ , and  $\Psi_L$  are the corresponding average fecal pellet sinking rates ( $m d^{-1}$ ), respectively.

Fecal pellet production experiments were carried out with the dominant copepod *Calanus sinicus* picked from the trawl net. A surface seawater sample from a bloom station containing many phytoplankton aggregates was diluted to different gradient concentrations (dilution factors were 1, 2, 4, 8, 16, and 32), and the particle sinking rates were measured in the SETCOL columns in triplicate. *Calanus sinicus* was allowed to feed in seawater from bloom stations diluted to different degrees with filtered seawater (triplicates). Fecal pellets excreted by *C. sinicus* were filtered onto a 10  $\mu m$  mesh net and then gently washed in distilled water. Fecal pellets were filtered onto a 60- $\mu m$  mesh and rinsed carefully with distilled water before being used to measure sinking rates and POC contents. Finally, the fecal pellets were filtered onto GF/F filters for fecal pellet POC analysis and estimation of fecal pellet production rates (Paffenhofer and Knowles, 1979; Marty et al., 2009). In situ zooplankton grazing rates were measured with the gut pigment method, which was initially reported by Mackas and Bohrer (1976) and subsequently improved by Wang and Conover (1986). According to the equations derived in those reports,

$$I = G \times r \quad (8)$$

where  $I$  is the grazing rates of the zooplankton,  $G$  is the evacuation rate, and  $r$  is the gut pigment content.

### 3. Results

#### 3.1. Phytoplankton abundance, Chl *a* concentration, and carbon biomass

The phytoplankton bloom we observed in the ECS lasted about one week, from 1 May 2016–6 May 2016. At both bloom and non-bloom stations, the temperature decreased gradually from the surface to a depth of 20 m; it then increased gradually to the bottom (15.6–19.7 °C, Fig. 2a, b); The salinity increased gradually with depth from the surface and reached a maximum at about 20 m (27.8–34.2, Fig. 2c, d). Maximum values of Chl *a* fluorescence at the study stations were observed at a depth of about 5 m. The range of Chl *a* at bloom stations and non-bloom reference stations were 0.4–56.6  $mg m^{-3}$  and 0.1–2.8  $mg m^{-3}$ , respectively (Fig. 3a, b). From the surface to a depth of about 20 m, the turbidity values were positively correlated with the Chl *a* concentrations, but turbidity increased abruptly at a depth of 20 m and remained high to the bottom (Fig. 3c, d). The surface phytoplankton cell abundance and Chl *a* concentration on 3 May 2016 during the bloom ECS2 were as high as  $18 \times 10^6$  cell  $L^{-1}$  and 58.1  $\mu g L^{-1}$ , respectively (Fig. 4a). These values were more than 20 times the corresponding values during the post-bloom period ( $860 \times 10^3$  cell  $L^{-1}$  and 2.57  $\mu g L^{-1}$ , respectively). Phytoplankton cell abundance and Chl *a* concentration during the bloom at bloom stations ECS1 and ECS2 were more than 10 times the corresponding values at non-bloom reference stations ECS3 and ECS4 ( $t$ -test,  $p < 0.05$ , Fig. 4c). Coincidentally, phytoplankton carbon biomass at bloom station ECS1 (average  $\pm$  SD,  $21 \pm 1 g C m^{-3}$ ) and ECS2 ( $24 \pm 1.4 g C m^{-3}$ ) were also more than 10 times the corresponding values at non-bloom stations ECS3 and ECS4 ( $t$ -test,

$p < 0.05$ ). *Prorocentrum donghaiense* (Dinoflagellates) was the dominant phytoplankton species at all stations during this study. *P. donghaiense* contributed up to 99% of the total phytoplankton cell abundance in the surface layer during the bloom (Fig. 4b). This percentage was significantly higher at the bloom stations ECS1 and ECS2 than at control stations ECS3 and ECS4 ( $t$ -test,  $p < 0.05$ ).

#### 3.2. Phytoplankton sinking rates and POC fluxes

During the bloom, the sinking rate ( $Y$ ) of phytoplankton increased with cell abundance ( $X$ ). The relationship was logarithmic and statistically significant [ $Y = 4.62 * \ln(X) - 32.59$ ,  $n = 42$ ,  $R^2 = 0.76$ ,  $p < 0.05$ , Fig. 5]. The maximum sinking rate was almost 16  $m d^{-1}$ , almost 100 times the sinking rate when cell abundance was low (0.17  $m d^{-1}$ , Fig. 5). The average sinking rate of phytoplankton during the bloom was more than 10 times the average rate at non-bloom stations,  $12.0 \pm 1.5$  and  $1.0 \pm 0.8 m d^{-1}$ , respectively (Fig. 8).

Microscopic analysis revealed that most *Prorocentrum donghaiense* cells in the bloom water had formed aggregations. The linear dimensions of the aggregations exceeded 400  $\mu m$ ; some were even macroscopic, with linear dimensions up to several centimeters (Fig. 6). Dilution of the surface bloom water by as much as a factor of 32 had no significant effect on the particle sinking rates ( $t$ -test,  $p > 0.05$ , Fig. 7). Based on Eqs. (1)–(5), the phytoplankton POC flux at bloom stations ECS1 and ECS2 were  $21 \pm 1.1$  and  $24 \pm 1.4 g C m^{-2} d^{-1}$ , respectively. These were about 100 times the fluxes at non-bloom stations ECS3 and ECS4 ( $0.26 \pm 0.04$  and  $0.21 \pm 0.03 g C m^{-2} d^{-1}$ ,  $t$ -test,  $p < 0.05$ ,  $n = 6$ , Fig. 8a). Phytoplankton POC fluxes contributed more than 90% and only 40% of the total POC fluxes at bloom and non-bloom stations, respectively (Fig. 8b). The contributions of phytoplankton POC flux to total POC flux were significantly different during different phases of the bloom ( $t$ -test,  $p < 0.05$ ) and varied from less than 40% to more than 90% of the total POC flux (about 0.3–24  $g C m^{-2} d^{-1}$ , Fig. 8c). Phytoplankton POC concentrations at depths of 5 m and 15 m (Fig. 9a) were more than 10 times the concentrations at a depth of 35 m at the bloom stations ECS1 and ECS2 (2.2–2.8  $g C m^{-3}$ , Fig. 9a). The sinking rates were obviously lower at a depth of 35 m (average sinking rates  $< 10 m d^{-1}$ ) than at 5 m and 15 m at (average sinking rates  $> 15 m d^{-1}$ ) the bloom stations (Fig. 9b,  $t$ -test,  $p < 0.05$ ). Based on phytoplankton POC content and sinking rates at 5 m, 15 m and 35 m, we estimated the POC fluxes in each water layer of bloom stations (Fig. 9c) and non-bloom stations (Fig. 9d) according to Eq. (5) and make a linear regression curve. The relationship between depth and phytoplankton POC flux was a binary linear equations regression curve in both bloom and non-bloom stations. The regression curve in the bloom stations and non-bloom station was  $y = -15.952x^2 + 30.529x + 41,192$ ,  $R^2 = 0.96$  and  $y = -0.287x^2 + 9.9296x + 239.4$ ,  $R^2 = 0.78$ , respectively.

#### 3.3. Zooplankton grazing rates and fecal pellet production rates

The copepod *Calanus sinicus* was the dominant species in the mesozooplankton community (in terms of both abundance and biomass) at bloom and non-bloom stations. The grazing rates and fecal pellet production rates of the large mesozooplankton ( $> 1000 \mu m$ ) were 208  $mg C m^{-3} d^{-1}$  and 141  $mg C m^{-3} d^{-1}$ , respectively, significantly higher than the corresponding rates for the other groups (Fig. 10). In addition, mesozooplankton grazing rates and fecal pellet production rates at bloom stations were significantly higher than the corresponding rates at non-bloom stations (Fig. 10a, b). The mesozooplankton grazing rates and fecal pellet production rates were therefore both enhanced by the increased phytoplankton cell abundance during the bloom. The results of the *C. sinicus* culture experiment were consistent with this observation (Fig. 10c). The significant decrease of the egestion rates and egestion-body ratios of *C. sinicus* with increasing dilution of the phytoplankton samples during the boom ( $p < 0.05$ ) indicated that there was a positive correlation between egestion rate and

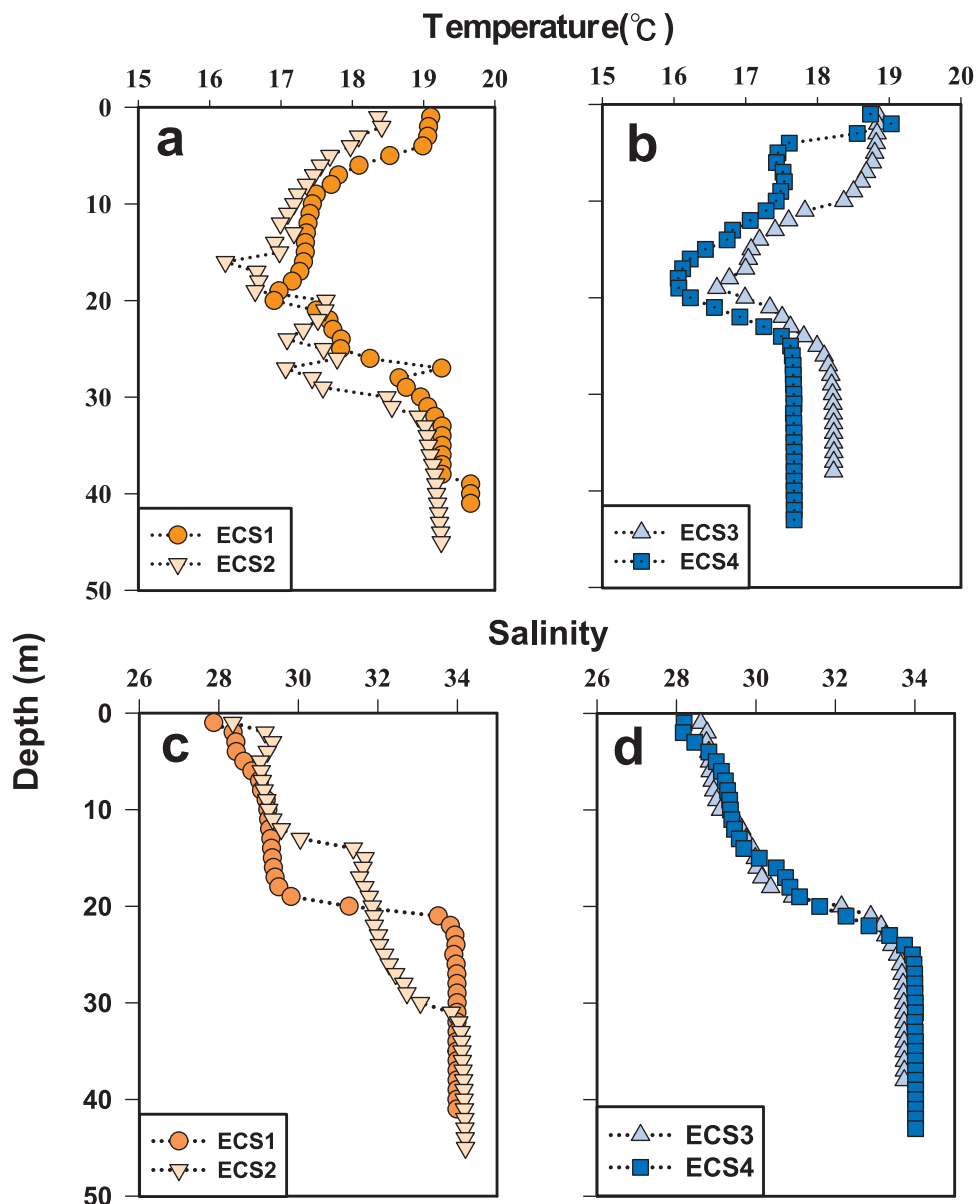


Fig. 2. Vertical CTD profiles of temperature and salinity. a) Temperature profiles at bloom stations ECS1 and ECS2; b) Temperature profiles at non-bloom stations ECS3 and ECS4; c) Salinity profiles at bloom stations ECS1 and ECS2; d) Salinity profiles at non-bloom stations.

phytoplankton abundance.

### 3.4. Zooplankton fecal pellet sinking rates, POC content, and POC fluxes

Zooplankton fecal pellet sinking rates ranged from 30 to 349  $\text{m d}^{-1}$  ( $192 \pm 86 \text{ m d}^{-1}$  in mean) at station ECS1 and from 41  $\text{m d}^{-1}$  to 320  $\text{m d}^{-1}$  ( $188 \pm 74 \text{ m d}^{-1}$  in mean) at station ECS2 during the bloom (Fig. 10a). The medium group (FP volume  $500\text{--}5000 \times 10^3 \mu\text{m}^3$ ) and large group fecal pellet (FP volume  $> 5000 \times 10^3 \mu\text{m}^3$ ) sinking rates were both significantly higher at the bloom stations than at the non-bloom stations (Fig. 11a). But the sinking rates of total zooplankton fecal pellets were not significantly higher at the bloom stations than at the non-bloom stations ( $n = 60, p > 0.05$ ). Those rates ranged from 32 to 280  $\text{m d}^{-1}$  (mean  $\pm$  SD:  $147 \pm 69 \text{ m d}^{-1}$ ) and 20–290  $\text{m d}^{-1}$  (mean  $\pm$  SD:  $140 \pm 77 \text{ m d}^{-1}$ ) at reference stations ECS3 and ECS4, respectively (Fig. 11a).

However, fecal pellet POC contents at the bloom stations were 3.4 and  $4.7 \text{ mg C m}^{-3}$ , about 3 times the content at non-bloom stations (1.4 and  $1.2 \text{ mg C m}^{-3}$ , Fig. 11b). Large-volume copepod fecal pellets with

the highest sinking rates were the most important contributor to the total fecal pellet POC content at both the bloom and non-bloom stations. The contributions of these large group fecal pellets to the total fecal pellet POC content exceeded 44% at both the bloom and non-bloom stations (Fig. 10b). These contributions were significantly higher than the contributions from the medium group and small group ( $t$ -test,  $p < 0.05$ , Fig. 11b). In addition, the contributions of large fecal pellets to the total fecal pellet POC fluxes were greater at the bloom stations than at the non-bloom stations, and the sinking rates were significantly higher as well (Fig. 11c). But the percentages of total POC content and total POC flux (including phytoplankton, fecal pellets, and other particulate debris) contributed by fecal pellets was significantly lower at bloom stations than at non-bloom stations (Fig. 12).

Similar to the phytoplankton fluxes, the zooplankton fecal pellet POC fluxes were estimated with Eqs. (6) and (7) from the sinking rates and POC contents. At bloom stations ECS1 and ECS2, these fluxes were 0.95 and  $1.4 \text{ g C m}^{-2} \text{ d}^{-1}$ , respectively, 4–6 times the values at non-bloom stations ECS3 ( $0.25 \text{ g C m}^{-2} \text{ d}^{-1}$ ) and ECS4 ( $0.20 \text{ g C m}^{-2} \text{ d}^{-1}$ ) ( $t$ -test,  $p < 0.05$ , Fig. 12c). At the non-bloom stations, the contributions

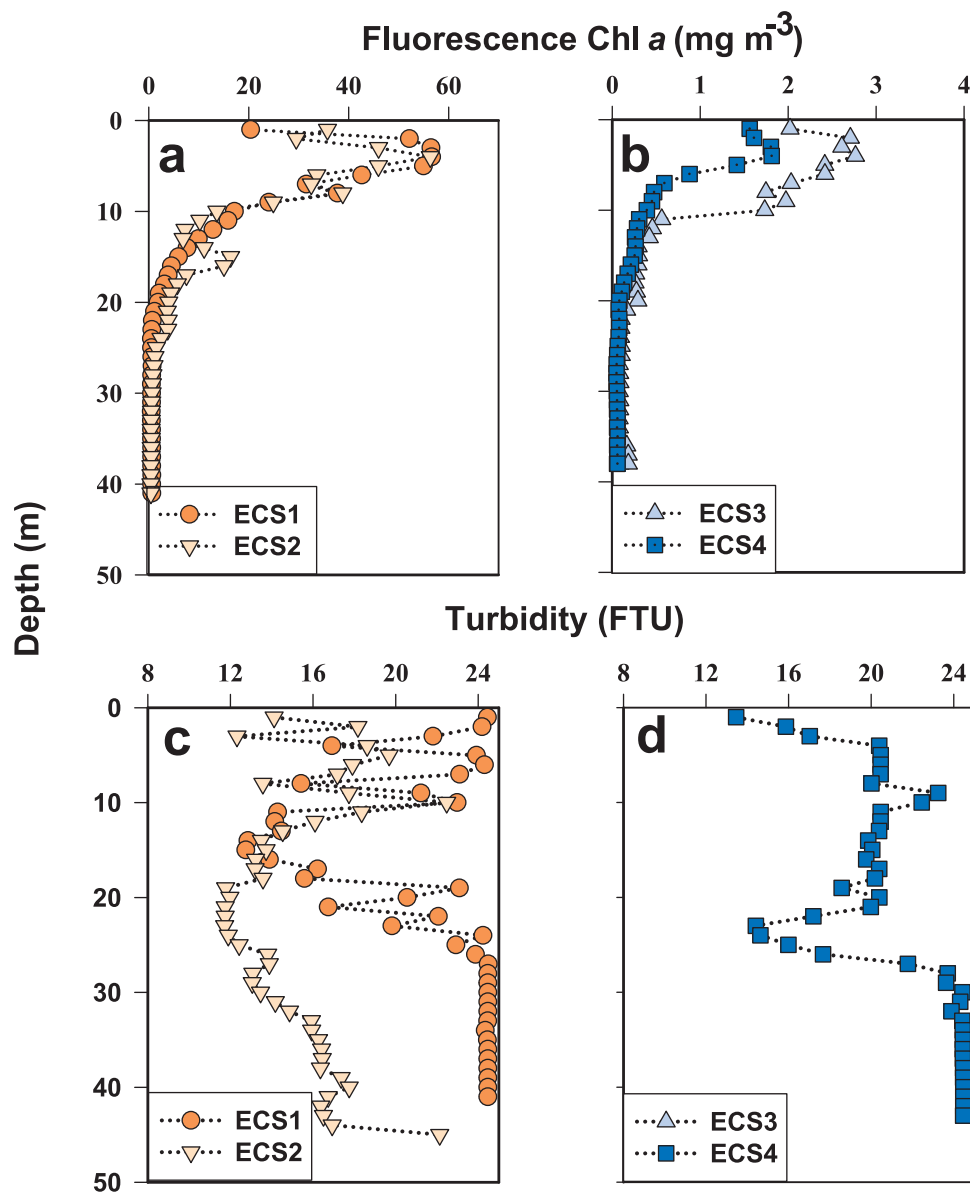


**Fig. 3.** CTD profiles of fluorescence Chl *a* and turbidity in study stations. a) Chl *a* profiles at bloom stations ECS1 and ECS2; b) Chl *a* profiles at non-bloom stations ECS3 and ECS4; c) Turbidity profiles at bloom stations ECS1 and ECS2; d) Turbidity profiles at non-bloom stations ECS3 and ECS4. Chl *a*: Chlorophyll *a*; Turbidity: Formazan Turbidity Unit.

of the fluxes of phytoplankton cells and zooplankton fecal pellets to the total POC flux were about 45% and 43%, respectively (Fig. 12b). The POC fluxes of both phytoplankton cells and zooplankton fecal pellets increased significantly at the bloom stations; however, the contribution of phytoplankton cells increased up to 95%, whereas that of fecal pellets decreased to less than 5% (Fig. 12b).

## 4. Discussion

### 4.1. Phytoplankton sinking rates

Our results revealed that the Chl *a* concentration and phytoplankton cell abundance were extremely high during the bloom (Table 1 and Fig. 4). Meanwhile, the phytoplankton sinking rates at bloom stations were more than 10 times the rates at non-bloom stations ( $p < 0.05$ , Fig. 5). The SETCOL method is a simple and reliable method that is suitable for both heterogeneous field populations and in vitro unialgal cultures and is based on a sound theoretical foundation (O'Brien et al., 2006; Bach et al., 2016). SETCOL is a member of the homogeneous-

sample family of methods (Bienfang et al., 1977). The procedure involves the use of settling columns of known height, initially containing a uniform distribution of cells. The population's mean sinking rate is calculated based on the change in the vertical distribution of biomass after a given time (Bienfang, 1981). The SETCOL sinking rate calculation methodology has currently been cited in 126 papers. Stokes derived an expression, now known as Stokes' law (Zwanzig, 1964), that suggests that particle sinking rates are regulated mainly by particle content and size. Although environmental changes affect cell size and composition, it is impossible for the individual cells of one species to undergo order-of-magnitude changes in both cell size and content during a bloom (Fig. 6). However, the sinking rates of particles can vary over several orders of magnitude because of differences of fluid viscosity, particle source material, morphology, porosity, and other variable particle characteristics (O'Brien et al., 2006; McDonnell, 2011). In the inner shelf of the ECS, diatoms and dinoflagellates are perennially the dominant taxa (Liu et al., 2016), especially *Skeletonema costatum* and *Prorocentrum dentatum*. The cell sizes of these two species are typically 4–12  $\mu\text{m}$  (Sarno et al., 2005) and 15–17  $\mu\text{m}$  (Lu et al., 2003),

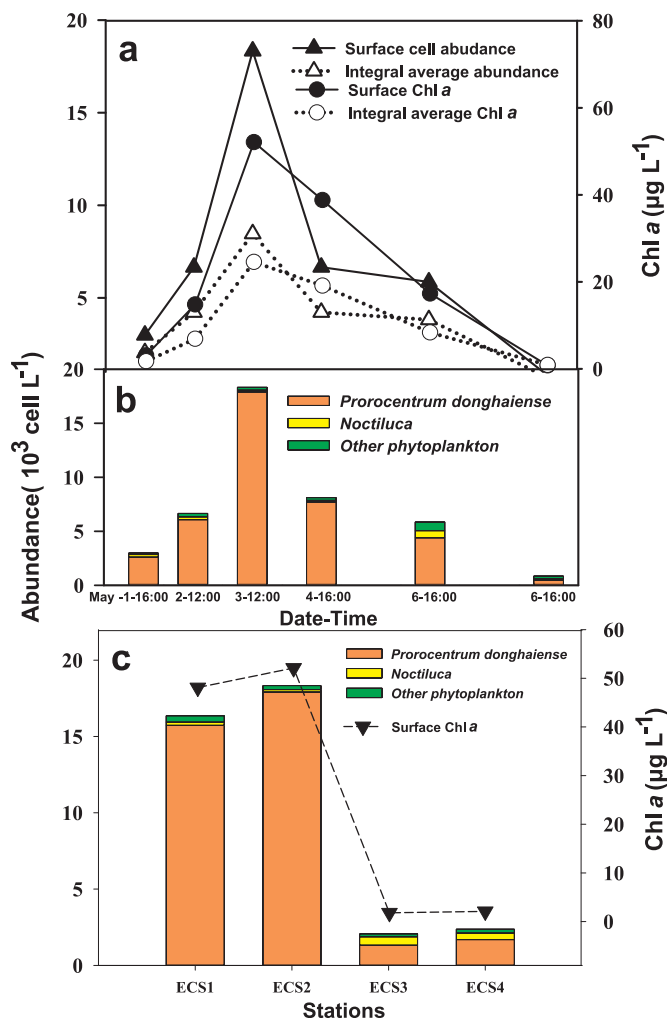


Fig. 4. Change of phytoplankton cell abundance and Chl a during a spring bloom in the ECS. a), b) Change of surface phytoplankton cell abundance process during the spring bloom in the bloom station ECS2. c) Phytoplankton surface cell abundance and Chl a in bloom stations (stations ECS1 and ECS2) and non-bloom reference stations (stations ECS3 and ECS4) in the East China Sea.

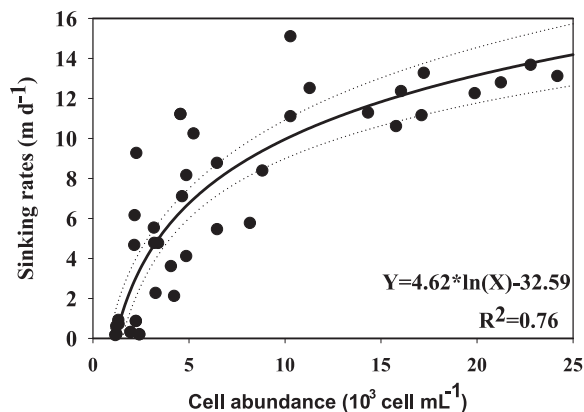


Fig. 5. Relationship between phytoplankton sinking rates and cell abundance ( $Y = 4.62 * \ln(X) - 32.59$ ,  $R^2 = 0.76$ ). Sinking rates of different phytoplankton cell abundance were from the bloom and non-bloom stations.

respectively. Phytoplankton sinking rates average  $0.13$  and  $1.71 \text{ m d}^{-1}$  when dinoflagellates and diatoms dominate the phytoplankton community in the ECS during the spring and summer, respectively (Guo

et al., 2016). We therefore suggest that the much higher sinking rates we observed during the bloom were a result of the extremely high cell abundance, which led to the aggregation of phytoplankton cells.

While they are growing, phytoplankton cells secrete a mucus composed of polysaccharides. The mucus is sticky and can bind the phytoplankton cells to form an aggregation (Passow, 2002). Some reports have indicated that *Prorocentrum* produces copious amounts of mucous that can form mucous plugs (Tang et al., 2008; Han et al., 2016) that would promote the formation of aggregates (Riemann, 1989). Indeed, our microscopic observations were consistent with this scenario; many cells formed aggregations that sank rapidly at bloom stations (Fig. 6). The positive correlation between phytoplankton sinking rates and cell abundances from different seawater samples (Fig. 5) does not conform to Stokes' law (Fowler and Small, 1972). Generally, the sinking rate of particles is independent of abundance. Moreover, the sinking rates of these particles were still very high, even when the bloom water was diluted by as much as a factor of 32 (Fig. 7). This result of the dilution experiments showed that phytoplankton sinking rate and cell abundance were related, not because of increased abundance but because the phytoplankton cells were aggregated.

The sinking rate calculated with Eq. (4) was based on the change in the vertical distribution of cells after a given time. The results are therefore not the sinking rates of individual phytoplankton cells but rather the average sinking rates of the phytoplankton community (McDonnell and Buesseler, 2012). In this study, the sinking rate of phytoplankton increased tenfold due to aggregation of phytoplankton cells. The implication is that phytoplankton did not sink as individual cells, but rather as aggregations. These results provide further indication that the *P. donghaiense* cells aggregated during the development of the bloom. In previous studies of aggregates, most of the aggregates ranged in size from  $0.4 \text{ mm}$  to a few tens of  $\text{mm}$ , and sinking rates ranged from tens to hundreds of meters per day (Shanks and Trent, 1980; Turner, 2015). Asper and Smith (2003) observed sinking rates of aggregates in the Ross Sea that equaled  $288 \text{ m d}^{-1}$ . Nowald et al. (2009) have also reported massive sinking of phytoplankton in the form of aggregates rather than individual cells at stations where blooms were occurring. We therefore hypothesize that at the bloom stations the formation of aggregates significantly increased the sinking rates of phytoplankton cells and promoted the export of phytoplankton POC. Our results are consistent with previous studies and indicate that aggregation was the cause of the rapid sinking of the phytoplankton cells (Figs. 5–7).

However, the cells within an aggregate are loosely packed, and the large amount of intercellular water reduces the average density of the phytoplankton aggregate. In fact, phytoplankton cells need to remain in the euphotic zone to receive adequate light for photosynthesis (Reynolds, 2006). Phytoplankton have therefore evolved over millennia in ways that tend to minimize sinking. The sinking rates of some diatoms, such as *Eucampia zodiacus* and *Rhizosolenia stoletiformis*, are inversely proportional to their chain lengths (Peperzak et al., 2003). Perhaps better known is the fact that *Trichodesmium thiebautii* can remain within the euphotic zone for long periods of time via the buoyancy provided by bubbles between filaments (Walsby, 1978). The consequences of aggregation may therefore differ as a function of the dominant species in a bloom. According to Stokes' law, when the effect of this density reduction is greater than the effect of the increase of volume, the phytoplankton sinking rate should decrease. However, if the phytoplankton aggregate adsorbs other high-density particles, the average density of the agglomerate will increase, and the sinking rate will increase. With few exceptions, aggregation is therefore an efficient way to increase the sinking rates of phytoplankton and their transport to the deep sea (Bach et al., 2016; Durkin et al., 2016).

#### 4.2. Phytoplankton POC flux

The ECS is a unique marginal sea that includes a large area of

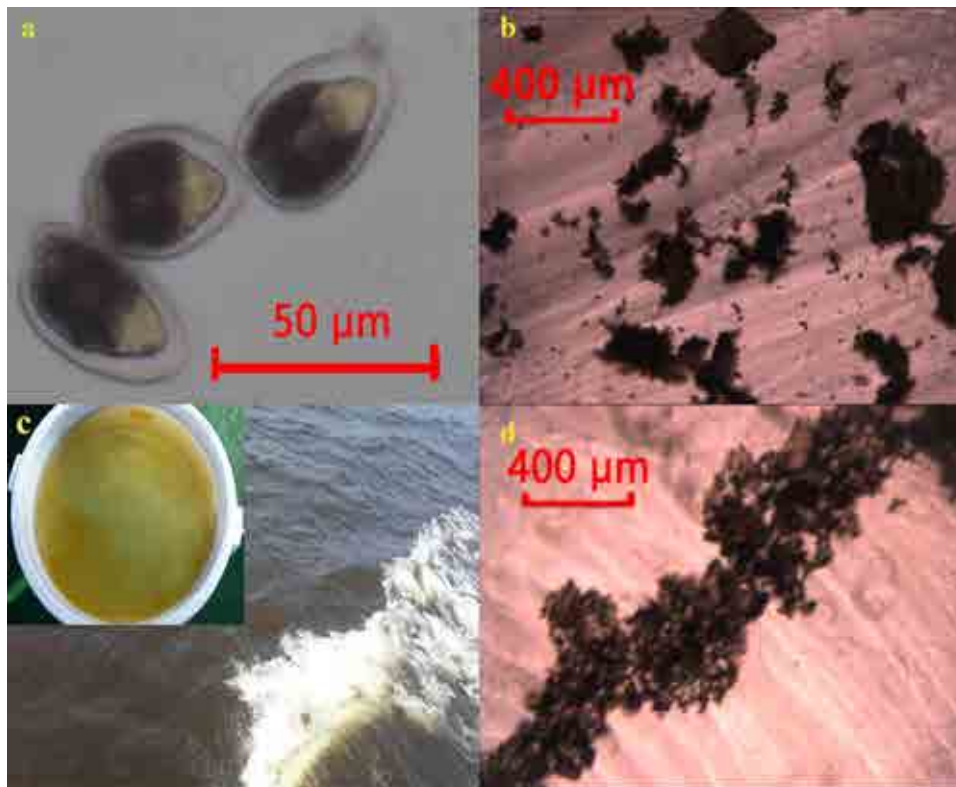


Fig. 6. In-situ phytoplankton samples photograph from bloom stations in the East China Sea, samples (*Prorocentrum donghaiense*) under 40× objective lens microscopy photograph (a), Under 5× objective lens microscopy photograph (b and d), and bloom seawater samples unaided eye photograph 1× by camera (c).

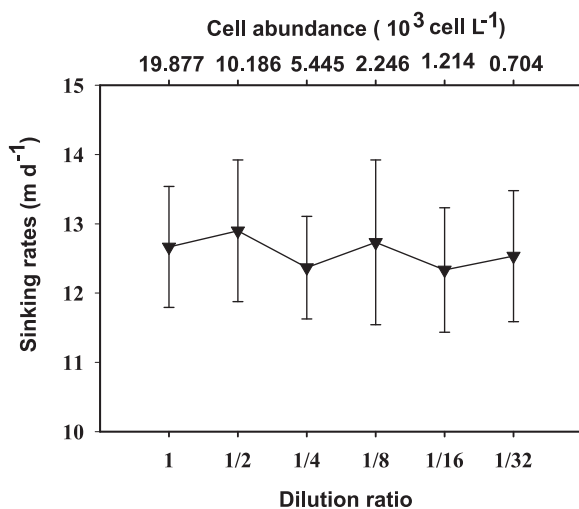
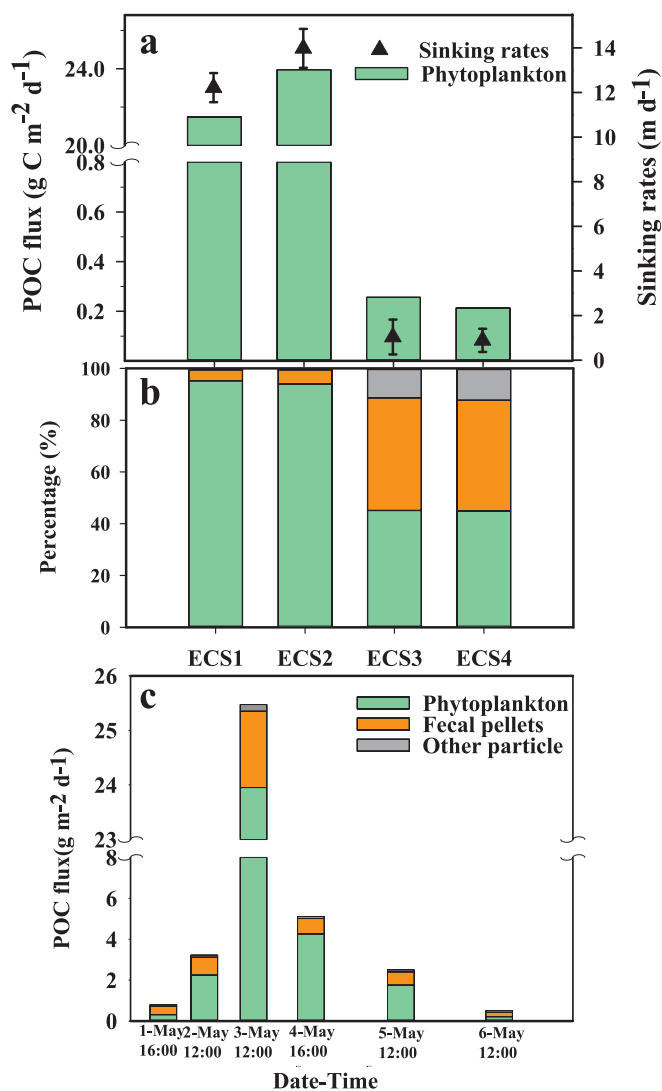


Fig. 7. Determination of sinking rates after different dilution ratio of the *Prorocentrum donghaiense* bloom seawater samples.

shallow continental shelf, with obvious effects of bottom resuspension (Pilskaln et al., 1998). Phytoplankton blooms vary greatly both in time and space within the inner shelf of the ECS. Although sediment traps are the most direct way to estimate the downward flux of particulate matter, POC fluxes estimated with sediment traps in shallow shelf waters can be seriously affected by resuspension of bottom sediment (Hung et al., 2013). In addition, in coastal waters there is a strong tidal current that can easily tilt the sediment trap and affect its collection efficiency (Gardner, 1985). More importantly, the bloom water mass can move horizontally, and the sediment trap may not be located in the area of the bloom throughout the bloom. The method of estimating POC fluxes in this study does not directly account for losses of POC through

solubilization and mineralization (Kjørboe et al., 1996). Nevertheless, according to Eq. (4), the POC content in estimating carbon flux is actually subtracted from the loss of POC. Guo et al. (2015) found that POC fluxes estimated from sediment traps and the SETCOL method were similar near our study area. Based on trap measurements and vertical mixing models, the POC export fluxes are 486–785  $\text{mg C m}^{-2} \text{ d}^{-1}$  in the coastal waters of the ECS (Hung et al., 2013). Hung et al. (2016) using the rare earth elements (REEs) mixing model found active sediment resuspension may significantly affect POC export flux (30–80%) in the East China Sea. Our results are consistent with this range of fluxes at the non-bloom stations (Table 1). The SETCOL method consequently can play an important role in estimating carbon fluxes in coastal areas during blooms. In addition, due to the shallowness of the water and short sinking time, any losses due to solubilization and mineralization during sinking can be neglected compared with the huge flux of sinking POC. The product of the POC concentration and sinking rate that we used to estimate the POC flux should therefore provide an accurate estimate of carbon fluxes in coastal areas during blooms.

Phytoplankton POC fluxes are usually less than  $10 \text{ mg C m}^{-2} \text{ d}^{-1}$  in the open ocean (Pesant et al., 2002) and tens to hundreds of  $\text{mg C m}^{-2} \text{ d}^{-1}$  in coastal areas (Smetacek et al., 1978; Peinert et al., 1982; Gowing et al., 2001; Pakhomov et al., 2002). Trap measurements and vertical mixing models indicate that POC export fluxes are 486–785  $\text{mg C m}^{-2} \text{ d}^{-1}$  in the coastal waters of the ECS (Hung et al., 2013). Our results are consistent with this range of fluxes at the non-bloom stations (Table 1). However, the phytoplankton POC fluxes were about  $24 \text{ g C m}^{-2} \text{ d}^{-1}$  at bloom stations (Fig. 8a), much greater than the range of fluxes previously reported in similar coastal waters (Table 1). Our results, however, are within the range of values reported from studies of sinking aggregates and marine snow (Asper, 1987; Alldredge and Gotschalk, 1988). In this study, the abundance of phytoplankton increased by roughly a factor of 10 during the *Prorocentrum donghaiense* bloom (Fig. 3b). In different areas of the ECS, the euphotic zone Chl *a* concentrations range from 1.6 to  $55.3 \mu\text{g L}^{-1}$  in spring, and the annual



**Fig. 8.** Comparison of phytoplankton POC flux estimated with SETCOL-measured sinking rates and POC content. a) Phytoplankton POC flux and sinking rates; b) the percentage of phytoplankton, fecal pellets and other particle to the total POC flux; c) Comparison changed of phytoplankton POC flux during the bloom process (From 16:00 1-May to 12:00 6-May).

average values range from 0.11 to 8.03  $\mu\text{g L}^{-1}$  (Gong et al., 2003). In this study, the Chl *a* concentrations at the bloom stations were as much as 58  $\mu\text{g L}^{-1}$ , dozens of times the average Chl *a* concentration reported in any previous study in non-bloom sea area (Liu et al., 2016). Furthermore, the sinking rates increased by more than a factor of ten because of aggregation (Figs. 5 and 6). Consequently, the phytoplankton POC fluxes were enhanced more than 100 times at the bloom stations as a result of the combined effects of the increases in both phytoplankton cell abundance/biomass and sinking rates (Fig. 8). A comparison with the phytoplankton C biomass indicates that the POC export flux was sufficient to completely deplete the phytoplankton C biomass in 3 days. But this very large POC flux was a very short-term event that exported POC that had accumulated over a longer period of time. It should be emphasized that the contribution of phytoplankton to the POC flux was greatly magnified because the export occurred at the end of a bloom. The POC fluxes at the bloom stations were extreme values in a small area in a short time interval during a particular event.

However, it is provocative to estimate the contribution of this episodic event to the annual POC flux. The blooms in the ECS can extend from the estuary of the Changjiang River down to the coastal waters of

Fujian Province. The area impacted by the blooms is more than 10,000  $\text{km}^2$ , and the blooms typically last for about 1 month from late April to early June (Tang et al., 2006). The primary production over the entire shelf of the ECS is quite high, 17–2079  $\text{mg C m}^{-2} \text{d}^{-1}$ , with an annual average of 145  $\text{g C m}^{-2} \text{yr}^{-1}$  (Gong et al., 2003). Because the ECS shelf is so productive, it has been regarded as an important sink of atmospheric  $\text{CO}_2$  (13.2  $\text{Tg C yr}^{-1}$ ) based on measurements of  $\text{CO}_2$  air-sea exchange (Guo et al., 2015). In the coastal area (41,000  $\text{km}^2$ ), the average  $\text{CO}_2$  flux from the atmosphere into the water during the spring is  $10.7 \pm 3.5 \text{ mmol m}^{-2} \text{d}^{-1}$ , and the annual amount of  $\text{CO}_2$  absorbed from the atmosphere is  $0.9 \pm 0.4 \text{ Tg C yr}^{-1}$  (Guo et al., 2015). The spring blooms have been reported in the ECS every year in the last decades and the blooms often spread to more than 1000  $\text{km}^2$  (Tang et al., 2006; Lou and Hu, 2014). The largest bloom on record occurred over an area of 10,000  $\text{km}^2$  in 2004. *Prorocentrum donghaiense* was dominant from 2000 to 2004 and has caused large blooms in May. If the bloom event that we observed occurred in an area of 1000  $\text{km}^2$  and lasted for about 7 days, the potential POC flux from this episodic event would have been 0.15  $\text{Tg C}$ , 17% of the  $\text{CO}_2$  sequestered from the atmosphere each year in the coastal zone of the ECS.

#### 4.3. Zooplankton fecal pellet sinking rates and POC fluxes

In this study, the fecal pellet sinking rates were 19.8–349  $\text{m d}^{-1}$  (Fig. 11a), within the range of previous reports (Yoon et al., 2001; Turner, 2002; Wilson et al., 2013). Overall, the average fecal pellet sinking rate during the bloom ( $191 \pm 77 \text{ m d}^{-1}$  in mean) was not significantly higher than the rate at non-bloom stations ( $143 \pm 73 \text{ m d}^{-1}$ ) (Fig. 11a). However, changes of the composition of the phytoplankton community can lead to changes of zooplankton diets (*Calanus sinicus* dominant), and the latter changes affect the rate of production and sinking characteristics of fecal pellets (Hansen et al., 1996a). Both the production rates and sizes of zooplankton fecal pellets are strongly dependent on the phytoplankton community (Haney and Trout, 1990). When *Acartia tonsa* was fed under simulated phytoplankton bloom conditions, its rate of fecal pellet production increased with increasing phytoplankton abundance (Butler and Dam, 1994). Bienfang (1980) have reported that herbivore diet affects zooplankton fecal pellet sinking rate. Fecal pellet length, width, volume, sinking rate would be change under different die populations. In this manuscripts, the sinking rates of zooplankton fecal pellets in bloom stations were not significantly higher than those in non-bloom stations, but the sinking rates of large size fecal pellets (volume >  $500 \times 103 \mu\text{m}^3$ ) were significantly higher than those in non-bloom stations.

Our results revealed that zooplankton ingestion and fecal pellet production rates increased during the bloom (Fig. 10). The result was a higher content of fecal pellet POC in the water compared to non-bloom stations (Fig. 11b). These results are consistent with previous reports of ingestion rates measured using the gut pigment content method during January off the Western Antarctic Peninsula (Gleiber et al., 2015). In addition, the production of more large fecal pellets (Fig. 11b) during the bloom indicates that high phytoplankton biomass could also alter the size distribution of the fecal pellets. There is no doubt that the greater number of large fecal pellets with faster sinking rates (Fig. 11a) significantly increased the POC flux (Fig. 11c). As Bienfang (1981) reported if no particle sink faster than  $l/t$ , and it has a negligible effect on sinking rates ( $\Psi$ ) for even somewhat longer periods than  $t$ , because the distribution of specific sinking velocities in populations shows an exponential-type decline in cohort fractions having rates considerably greater than the mean. It has been noted that when the sinking rate of fecal pellets is higher than  $l/t$ , the sinking rate may be some underestimation.

Overall, the fecal pellet POC flux during the bloom was enhanced because higher zooplankton grazing rates led to higher rates of fecal pellet production and higher fecal pellet POC content (Fig. 10). However, because of the much greater increase of the flux of sinking

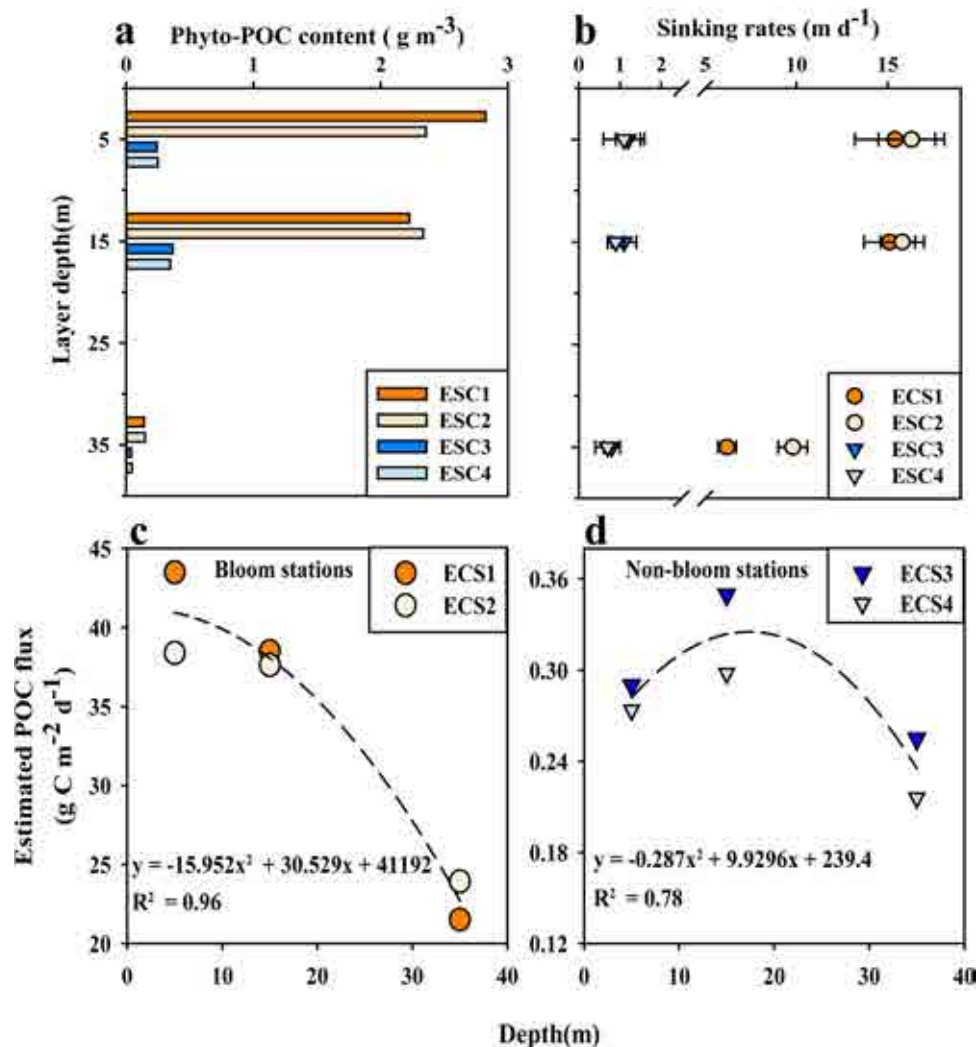


**Fig. 9.** Phytoplankton POC content (a) and sinking rates; (b) in 5 m, 15 m, 35 m layers at bloom stations. Phytoplankton POC content (a) and sinking rates; (b) in 5 m, 15 m, 35 m layers at bloom stations. The regression curve of the relationship between depth and phytoplankton POC flux in bloom (c) and non-bloom reference stations (d). Phyto-POC: phytoplankton particulate organic carbon.

phytoplankton cells, the relative proportion of fecal pellets to the total flux decreased to less than 5% during the bloom (Fig. 11b). Because the estimates of these two fluxes were carried out simultaneously, it is possible that a time lag in the production of fecal pellets may have caused the impact of the bloom on the flux of fecal pellets to be underestimated. For example, Butler and Dam (1994) have reported a significant increase of fecal pellet POC fluxes between early-bloom and late-bloom conditions,  $37 \text{ mg C m}^{-2} \text{ d}^{-1}$  and  $500 \text{ mg C m}^{-2} \text{ d}^{-1}$ , respectively, based on a compilation of results obtained using the same methods as this study. Moreover, the exports of phytoplankton cells and zooplankton pellets are not independent. Because the zooplankton pellet samples were trawled up from 35 m in this study, the results in Fig. 3 imply that the POC flux of zooplankton fecal pellets would be overestimated due to the influence of resuspension at both bloom station and reference non-bloom stations. The increased biological production during a bloom can trigger the production of transparent exopolymer particles (Passow, 2002), which can cause phytoplankton cells and detrital particles to aggregate into much larger particles (Wilson et al., 2008). In the open ocean, the material that can potentially form aggregates is very extensive and includes phytoplankton cells, zooplankton fecal pellets, mucus, detritus, and other particles (Hansen et al., 1996b; Alldredge et al., 2002). In addition, zooplankton fecal pellets not only increase the size and sinking rates of aggregations, but if the aggregates are consumed by larger zooplankton, the POC may be

repackaged into even larger fecal pellets with faster sinking rates (Vaillancourt et al., 2003).

#### 4.4. Effects of particles degradation and bottom resuspension on measured sinking rates and estimated POC

The SETCOL method using a 60-cm column to measure sinking rates of phytoplankton assemblages, aggregates, and fecal pellets on a short time scale. It may overestimate sinking rates to the extent that particles become smaller because of microbial degradation. Indeed, the faster the sinking rate, the shorter time a particle stays in the upper water column where degradation occurs most rapidly. The magnitude of the POC vertical flux is determined by the difference between the sinking velocity and the degradation rate of the sinking aggregates. Microbial degradation rates in terms of microbial carbon-specific respiration rates for a range of different particle types from the surface ocean seem to be converging on  $\sim 13\% \text{ d}^{-1}$  (Ploug et al., 2008; Neuer et al., 2004). The magnitude of microbial degradation in the upper ocean is determined mainly by the retention time of the aggregates, i.e. their sinking velocities (Neuer et al., 2004). In this study, the sinking rate of phytoplankton increased by 10 times compared to non-bloom stations due to the aggregation of phytoplankton cells. Such phytoplankton aggregates may even absorb additional particles during the sinking process and thereby increase their volume and sinking rate. In such a shallow area,

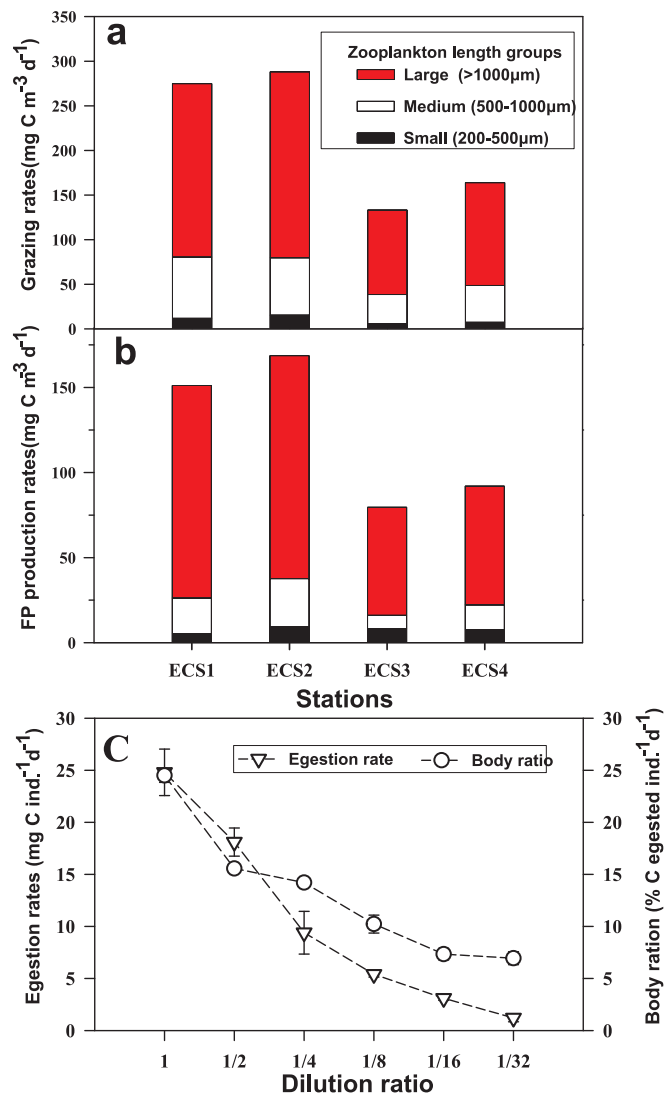


**Fig. 10.** Comparison of different length group zooplankton grazing rate, egestion rates between bloom stations and reference stations. a). and b). Zooplankton grazing rates and fecal pellets production separately. c) The egestion: body ratio of zooplankton, which were fed in different dilution ratio of bloom surface seawater phytoplankton samples.

such a rapid sinking rate will minimize the effects of degradation.

In order to assess the effect of resuspension on the phytoplankton and zooplankton samples obtained from the water column, we compared the vertical profiles of Chl *a* fluorescence and turbidity at the study stations (Fig. 3). The Chl *a* fluorescence was significantly higher in the upper 15 m than in waters below 15 m at both bloom and non-bloom stations (*t*-test, *p* < 0.001). The vertical profiles of turbidity, however, displayed two peaks at the bloom stations. The good correspondence between the upper peak and the high Chl *a* concentrations in the upper 15 m indicated the upper peak was contributed mainly by the increase of phytoplankton abundance. The lower peak, which increased from about 20 m and extended to the bottom, was probably the result of resuspension at depths below 20 m. We estimated POC fluxes by using the integral average POC content at 5 m, 15 m, and 35 m multiplied by the average sinking rates at those depths (Eq. (5)). Consistent with the Chl *a* results, phytoplankton POC concentrations were more than 10 times higher at 5 m and 15 m than at 35 m (Fig. 9a). In contrast, the sinking rates were clearly slower at 35 m than at 5 m and 15 m at the bloom stations (Fig. 9b, *t*-test, *p* < 0.05). Therefore, the POC concentrations at 5 m and 15 m made by far the most important

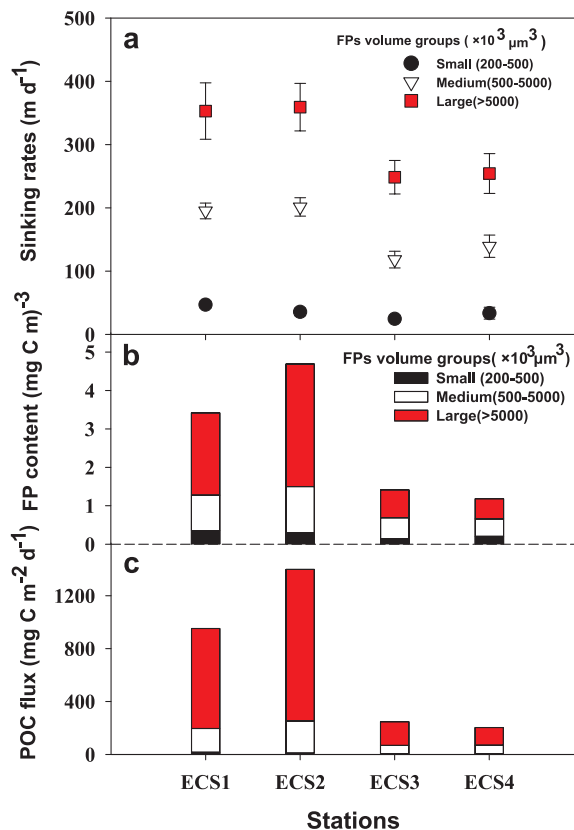


**Fig. 11.** Comparison of zooplankton fecal pellets sinking rates, POC content and POC flux between bloom stations and reference stations. a). Fecal pellets mean sinking rates and mean POC content. b). Fecal pellets sinking rates and mean POC content in different size group. c). Fecal pellets mean POC flux.

contribution to the export flux of the whole water column. The overall impact of resuspension on the calculated export flux was therefore very small. Fig. 9c and d showed that the relationship between depth and estimated phytoplankton POC flux was binary linear equations in both bloom and non-bloom stations. The results showed that when phytoplankton was sinking exported into the water layer below 35 m, the phytoplankton POC flux would decrease and significantly less than that in upper 35 m water layer. In addition, the actual POC flux in 35 m layer may be lower due to the strong resuspension effect on the bottom. Nonetheless, the potential contribution of phytoplankton POC to the export flux at bloom stations were still significantly higher than that of non-algal blooms (Fig. 9c, d).

#### 4.5. Effect of swimming behavior of *Prorocentrum donghaiense* on measured sinking rates

To meet their physiological requirements, individual dinoflagellates can meet their requirements for nutrients and light by swimming down and up, respectively (Smayda, 1997). The swimming speeds of dinoflagellates, up to 31 m d<sup>-1</sup> (Kamykowski et al., 1989), allow dinoflagellates to exploit the nutrient resource gradient and other microhabitat features (Smayda, 1997). Here we discuss the effect of the dinoflagellate's (*P. donghaiense*) swimming behavior on the sinking rates measured with SETCOL.

First, the swimming ability of a dinoflagellate may cause its sinking rate to be lower than that of other phytoplankton of a similar size at non-bloom stations. In this study, the four stations were all dominated by dinoflagellates (Fig. 4), and the phytoplankton sinking rates at non-bloom stations were < 1 m d<sup>-1</sup> (Fig. 8), lower than that of diatom-dominated communities (0–3.05 m d<sup>-1</sup>) (Waite et al., 1992a, 1992b). Based on laboratory tests, Pitcher and Mitchell-Llnes (1989) concluded

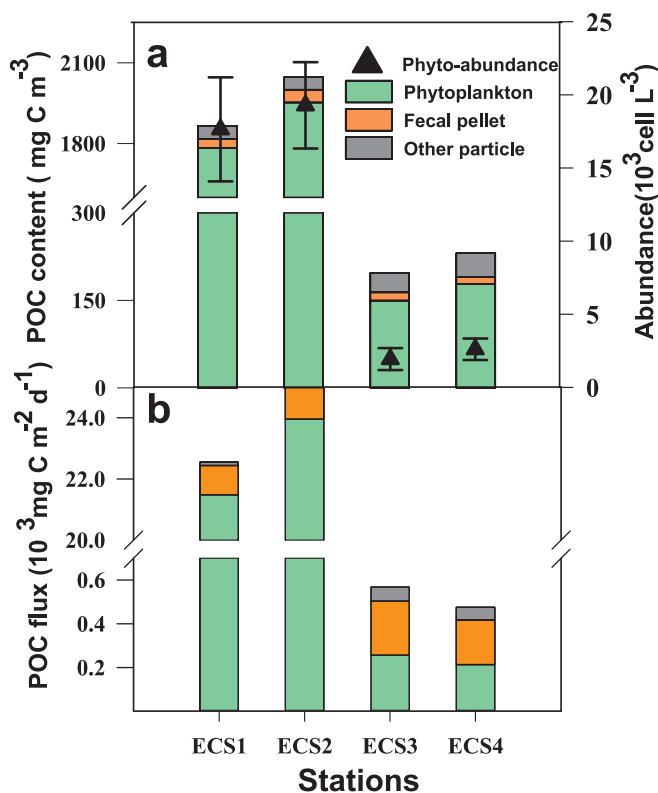


Fig. 12. Comparison of POC content and POC flux between bloom stations and reference stations. Fecal pellets and other particles were pick up from net, phytoplankton POC content and POC flux estimated from seawater samples.

that when the phytoplankton community is dominated by dinoflagellates, sinking rates are lower than when diatoms dominate. In contrast, during the late stages of a phytoplankton blooms, the surface water becomes depleted in nutrients. The downward swimming behavior of dinoflagellates in the late stages of a *P. donghaiense* bloom would cause the downward movement of the cells to exceed the sinking rates at bloom stations. Therefore, the downward swimming behavior of dinoflagellates may increase the measured sinking rate during the late stages of an algal bloom. However, the water in our SETCOL columns was well mixed; there was no nutrient gradient in the SETCOL columns. Therefore, the effective sinking rate of the phytoplankton may have been higher than the sinking rate we measured.

Second, in this study the dominant dinoflagellates, *P. donghaiense*, were concentrated into aggregates and therefore had lost any ability to

swim freely during the bloom (Fig. 6). The abundances of phytoplankton in the seawater at the bloom stations were as high as  $20 \times 10^3$  cells  $\text{mL}^{-1}$ . Microscopic observations showed that *P. donghaiense* was not present in the form of individual cells but instead was aggregated into large floc aggregates. In the floc aggregates, the dinoflagellates could no longer swim freely or may have already died (Fig. 6). In addition, individual dinoflagellates cells that are swimming freely may be more easily aggregated by sticky, sinking aggregates (Hansen et al., 1996b). The result would be an increase of the density of aggregates and further increase of their sinking rates.

Third, because the depths at all stations were  $< 50$  m (Fig. 1), it would have been impossible for dinoflagellates to swim either upward or downward continuously for even two days at  $31 \text{ m d}^{-1}$ . It is therefore reasonable to assume that the dinoflagellates were swimming both up and down. We would therefore expect that the average rate of vertical movement of the motile dinoflagellates was close to zero. Bienfang et al. (1977) argued that the sinking rate measured by SETCOL is the ecologically relevant sinking rate because it implicitly assigns a sinking rate of zero to all positively buoyant cells. Because the height of the SETCOL columns was 0.6 m, cells sinking at  $12 \text{ m d}^{-1}$  would sink from the top to the bottom in about 72 min. Dinoflagellates swimming at  $31 \text{ m d}^{-1}$  (Kamykowski et al., 1989) could swim from the top to the bottom of the column in about 28 min. They would then have to either turn around and swim upward or stop swimming. Our assessment is therefore that the swimming ability of the dinoflagellates actually helps to explain our experimental results.

## 5. Conclusions

In this paper, we studied the sinking rates of phytoplankton cells, zooplankton fecal pellets, and the potential fluxes of POC during a spring *P. donghaiense* bloom in the coastal area of the ECS. The total POC fluxes associated with both phytoplankton cells and zooplankton fecal pellets significantly increased during the bloom. The phytoplankton POC flux, in particular, showed an unexpectedly large increase because of the enhancement of both the sinking rates and concentration of POC. The phytoplankton sinking rates were faster than anticipated, mainly because the cells were repackaged into aggregates with sizes larger than 4 mm at coastal bloom stations. In the meantime, the dramatic increase of phytoplankton biomass changed the zooplankton diet during the bloom process. Zooplankton ingestion rates and fecal pellet production rates were enhanced, and the fecal pellet POC flux significantly increased, mainly because of the increase of their POC content. The majority of the total sinking POC came directly from phytoplankton. Such dramatic, albeit brief, events may make a very important potential contribution to the annual POC flux. If the bloom event that we observed occurred in an area of  $1000 \text{ km}^2$  and lasted for

Table 1  
Summary phytoplankton POC flux in difference marine environment.

Location	Dominant Phytoplankton	Chl <i>a</i> ( $\mu\text{g L}^{-1}$ )	POC flux ( $\text{mg C m}^{-2} \text{ day}^{-1}$ )	Bloom/non-bloom	Method	Reference
East China Sea	Coast	Dinoflagellates( <i>Prorocentrum donghaiense</i> )	52.1	$24.0 \times 10^3, 21.5 \times 10^3$	Bloom	SETCOL This study
	Coast	Dinoflagellates( <i>Prorocentrum donghaiense</i> )	$< 1$	256, 213	Non-bloom	SETCOL This study
	Coast	Diatom/ Dinoflagellates ( <i>Skeletonema dornhii/ Prorocentrum dentatum</i> )	30.2	$63.13 \pm 48.16$	Bloom	SETCOL (Guo et al., 2016)
Coast	Diatom( <i>Skeletonema costatum</i> )	0.3–8.9	$785 \pm 438$	Non-bloom	Trap	(Hung et al., 2013)
	Outer Shelf	Pico-phytoplankton		$58 \pm 33$		
Atlantic coast	Coast	Diatom/ Dinoflagellates	$< 4$	48–292	Non-bloom	Traps (Hung et al., 2016)
	Coast	<i>Chaetoceros</i> spp. Diatom	20	10–200	Bloom:	SETCOL (Kjorboe et al., 1996)
Southern Ocean	The Lazarev Sea	Flagellates(nano- and pico-size classes)	0.8–1.6	24–48	Non-bloom	Trap (Pakhomov et al., 2002)
	The Ross Sea	Haptophyte, Diatom( <i>Phaeocystis Antarctica</i> )	–	4.5–21.1	Non-bloom	Trap (Gowing et al., 2001)
Baltic Sea.	Kiel Bight	Diatom( <i>Detonula confervacea</i> )	$< 20.5$	460	Bloom	Trap (Peinert et al., 1982)
	Bornholm Basin	Diatom( <i>Skeletonema costatum</i> )	3.6	182.35	Bloom	Trap (Smetacek et al., 1978)
Greenland Sea	Polynya	Diatom( <i>Phaeocystis Antarctica</i> )	$< 3$	0.27–2.94	Non-bloom	SETCOL (Pesant et al., 1998)

about 7 days, the potential POC flux from this episodic event would have been 0.15 Tg C, 17% of the CO<sub>2</sub> sequestered from the atmosphere each year in the coastal zone of the ECS.

## Acknowledgements

We thank Wupeng Xiao, Zhen Cao and Lei Wang for analyzing chlorophyll a data. We also thank Yibin Huang and Changlin Li for their helpful comments and suggestions on this manuscript. We would like to thank the captains and crew of the “Yanping 2”, who made concerted efforts to assist during field sampling.

## Funding

This work was supported by grants from the China NSF Key Project (No. 41330961), the National Key Research and Development Program of China (No. 2016YFA0601201), and partially from the others National Natural Science Foundation of China (Nos. 41776146 and U1406403).

## References

- Allredge, A.L., Gotschalk, C., 1988. In situ settling behavior of marine snow. *Limnol. Oceanogr.* 33, 339–351.
- Allredge, A.L., Cowles, T.J., MacIntyre, S., Rines, S., Donaghay, J.E.B., Greenlaw, P.L., Holliday, C.F., D. V., et al., 2002. Occurrence and mechanisms of formation of a dramatic thin layer of marine snow in a shallow Pacific fjord. *Mar. Ecol. Prog. Ser.* 233, 1–12.
- Asper, V.L., 1987. Measuring the flux and sinking speed of marine snow aggregates. *Deep Sea Res. Part A Oceanogr. Res. Pap.* 34, 1–17.
- Asper, V.L., Smith, W.O., 2003. Abundance, distribution and sinking rates of aggregates in the Ross Sea, Antarctica. *Deep Sea Res. Part I: Oceanogr. Res. Pap.* 50, 131–150.
- Bach, L.T., Boxhammer, T., Larsen, A., Hildebrandt, N., Schulz, K.G., Riebesell, U., 2016. Influence of plankton community structure on the sinking velocity of marine aggregates. *Glob. Biogeochem. Cycles* 30, 1145–1165.
- Belcher, A., Iversen, M., Manno, C., Henson, S.A., Tarling, G.A., Sanders, R., 2016. The role of particle associated microbes in remineralization of fecal pellets in the upper mesopelagic of the Scotia Sea, Antarctica. *Limnol. Oceanogr.* 61, 1049–1064.
- Bienfang, P.K., 1980. Phytoplankton sinking rates in oligotrophic waters off Hawaii, USA. *Mar. Biol.* 61, 69–77.
- Bienfang, P.K., 1981. Setcol - a technologically simple and reliable method for measuring phytoplankton sinking rates. *Can. J. Fish. Aquat. Sci.* 38, 1289–1294.
- Bienfang, P.K., Laws, E., Johnson, W., 1977. Phytoplankton sinking rate determination: technical and theoretical aspects, an improved methodology. *J. Exp. Mar. Biol. Ecol.* 30 (3), 283–300.
- Butler, M., Dam, H.G., 1994. Production rates and characteristics of fecal pellets of the copepod *Acartia tonsa* under simulated phytoplankton bloom conditions: implications for vertical fluxes. *Mar. Ecol. Prog. Ser.* 114, 81–91.
- Chen, C.-T.A., Wang, S.-L., 1999. Carbon, alkalinity and nutrient budgets on the East China Sea continental shelf. *J. Geophys. Res.: Oceans* 104, 20675–20686.
- Dagg, M.J., Jackson, G.A., Checkley, D.M., 2014. The distribution and vertical flux of fecal pellets from large zooplankton in Monterey bay and coastal California. *Deep Sea Res. Part I: Oceanogr. Res. Pap.* 94, 72–86.
- Durkin, C.A., Van Mooy, B.A.S., Dyrhman, S.T., Buesseler, K.O., 2016. Sinking phytoplankton associated with carbon flux in the Atlantic Ocean. *Limnol. Oceanogr.* 61, 1172–1187.
- Ebersbach, F., Assmy, P., Martin, P., Schulz, I., Wolzenburg, S., Nöthig, E.-M., 2014. Particle flux characterisation and sedimentation patterns of protistan plankton during the iron fertilisation experiment LOHAFEX in the Southern Ocean. *Deep Sea Res. Part I: Oceanogr. Res. Pap.* 89, 94–103.
- Eppey, R.W., Reid, F.M.H., Strickland, J.D.H., 1970. Estimates of Phytoplankton Crop Size, Growth Rate, and Primary Production (Ph.D. Thesis). Calif Univ Scripps Inst Oceanogr Bull.
- Gleiber, M.R., Steinberg, D.K., Schofield, O.M., 2015. Copepod summer grazing and fecal pellet production along the Western Antarctic Peninsula. *J. Plankton Res.* 38, 732–750.
- Gong, G.C., Wen, Y.H., Wang, B.W., Liu, G.J., 2003. Seasonal variation of chlorophyll a concentration, primary production and environmental conditions in the subtropical East China Sea. *Deep Sea Res. Part II: Top. Stud. Oceanogr.* 50, 1219–1236.
- Gowing, M.M., Garrison, D.L., Kunze, H.B., Winchell, C.J., 2001. Biological components of Ross Sea short-term particle fluxes in the austral summer of 1995–1996. *Deep-Sea Res. Part I-Oceanogr. Res. Pap.* 48, 2645–2671.
- Guo, S.J., Feng, Y.Y., Wang, L., Dai, M.H., Liu, Z.L., Bai, Y., Sun, J., 2014b. Seasonal variation in the phytoplankton community of a continental-shelf sea: the East China Sea. *Mar. Ecol. Prog. Ser.* 516, 103–126.
- Guo, S.J., Sun, J., Zhao, Q.B., Feng, Y.Y., Huang, D.J., Liu, S.M., 2016. Sinking rates of phytoplankton in the Changjiang (Yangtze River) estuary: a comparative study between *Prorocentrum dentatum* and *Skeletonema dorhnii* bloom. *J. Mar. Syst.* 154, 5–14.
- Guo, X., Zhang, Y., 2005. Particle flux through the Huanghai Sea cold water mass. *Acta Oceanol. Sin.* 24, 78–88.
- Guo, X., Zhang, Y., Zhang, F., Cao, Q., 2010. Characteristics and flux of settling particulate matter in neritic waters: the southern Yellow Sea and the East China Sea. *Deep Sea Res. Part II: Top. Stud. Oceanogr.* 57, 1058–1063.
- Guo, X.H., Zhai, W.D., Dai, M.H., Zhang, C., Bai, Y., Xu, Y., Li, Q., et al., 2015. Air-sea CO<sub>2</sub> fluxes in the East China Sea based on multiple-year underway observations. *Biogeosciences* 12, 5495–5514.
- Gutiérrez-Rodríguez, A., Latasa, M., Estrada, M., Vidal, M., Marrasé, C., 2010. Carbon fluxes through major phytoplankton groups during the spring bloom and post-bloom in the Northwestern Mediterranean Sea. *Deep Sea Res. Part I: Oceanogr. Res. Pap.* 57, 486–500.
- Han, M.S., Wang, P., Kim, J.H., Cho, S.Y., Park, B.S., Kim, J.H., Katano, T., et al., 2016. Morphological and molecular phylogenetic position of *Prorocentrum micans* sensu stricto and description of *Prorocentrum koreanum* sp. nov. from Southern Coastal Waters in Korea and Japan. *Protist* 167, 32–50.
- Haney, J.F., Trout, M.A., 1990. Relationships between fecal pellet production and feeding in the calanoid copepod *Boeckella*. *J. Plankton Res.* 12, 701–716.
- Hansen, B., Fotel, F.L., Jensen, N.J., Madsen, S.D., 1996a. Bacteria associated with a marine planktonic copepod in culture. II. Degradation of fecal pellets produced on a diatom, a nanoflagellate or a dinoflagellate diet. *J. Plankton Res.* 18, 275–288.
- Hansen, J.L.S., Kjørboe, T., Allredge, A.L., 1996b. Marine snow derived from abandoned larvacean houses: sinking rates, particle content and mechanisms of aggregate formation. *Mar. Ecol. Prog. Ser.* 141, 205–215.
- Honjo, S., Eglinton, T., Taylor, C., Ulmer, K., Sievert, S., Bracher, A., German, C., et al., 2014. Understanding the role of the biological pump in the global carbon cycle: an imperative for ocean science. *Oceanography* 27, 10–16.
- Hoshika, A., Tanimoto, T., Mishima, Y., Iseki, K., Okamura, K., 2003. Variation of turbidity and particle transport in the bottom layer of the East China Sea. *Deep-Sea Res. Part II* 50, 443–455.
- Hung, C.C., Tseng, C.W., Gong, G.C., Chen, K.S., Chen, M.H., Hsu, S.C., 2013. Fluxes of particulate organic carbon in the East China Sea in summer. *Biogeosciences* 10, 6469–6484.
- Hung, C.C., Chen, Y.F., Hsu, S.C., Wang, K., Chen, J., Burdige, D.J., 2016. Using rare earth elements to constrain particulate organic carbon flux in the East China Sea. *Sci. Rep.* 6, 33880.
- Hung, C.-C., Gong, G.-C., 2011. Biogeochemical responses in the southern East China Sea after typhoons. *Oceanography* 24, 42–51.
- Hung, J.-J., Lin, C.S., Hung, G.W., Chung, Y.C., 1999. Lateral transport of lithogenic particles from the continental margin of the southern East China Sea. *Estuar. Coast. Shelf S.* 49, 483–499.
- Iseki, K., Okamura, K., Kiyomoto, Y., 2003. Seasonality and composition of downward particulate fluxes at the continental shelf and Okinawa Trough in the East China Sea. *Deep Sea Res. Part II: Top. Stud. Oceanogr.* 50, 457–473.
- Kamykowski, D., McCollum, S.A., Kirkpatrick, G., 1989. A comparison of the environmentally modulated swimming behavior of several photosynthetic marine dinoflagellates. *Red Tides: Biol. Environ. Sci. Toxicol.* 277–280.
- Kjørboe, T., Hansen, J.L.S., 1993. Phytoplankton aggregate formation: observations of patterns and mechanisms of cell sticking and the significance of exopolymeric material. *J. Plankton Res.* 15, 993–1018.
- Kjørboe, T., Hansen, J.L., Allredge, A.L., Jackson, G.A., Passow, U., Dam, H.G., Drapeau, D.T., et al., 1996. Sedimentation of phytoplankton during a diatom bloom: rates and mechanisms. *J. Mar. Res.* 54, 1123–1148.
- Le Quéré, C., Moriarty, R., Andrew, R.M., Canadell, J.G., Sitch, S., Korsbakken, J.I., Friedlingstein, P., et al., 2015. Global carbon budget 2015. *Earth Syst. Sci. Data* 7, 349–396.
- Le Quéré, C., Andrew, R.M., Canadell, J.G., Sitch, S., Korsbakken, J.I., Peters, G.P., Manning, A.C., et al., 2016. Global carbon budget 2016. *Earth Syst. Sci. Data* 8, 605–649.
- Liu, H.B., Wu, C.J., 2016. Effect of the silica content of diatom prey on the production, decomposition and sinking of fecal pellets of the copepod *Calanus sinicus*. *Biogeosciences* 13.
- Liu, K., Chao, S., Marra, J., Snidvongs, A., 2006. Monsoonal forcing and biogeochemical environments of outer southeast asia seas. *Sea* 14, 673–721.
- Liu, X., Xiao, W., Landry, M.R., Chiang, K.-P., Wang, L., Huang, B., 2016. Responses of phytoplankton communities to environmental variability in the East China Sea. *Ecosystems* 19, 832–849.
- Lou, X., Hu, C., 2014. Diurnal changes of a harmful algal bloom in the East China Sea: observations from GOCI. *Remote Sens Environ.* 140, 562–572.
- Lu, S., Zhang, Y., Chen, J., 2003. Scanning electron-microscopic study on *Prorocentrum dentatum* from the East China Sea. *Chin. J. Appl. Ecol.* 14, 1070.
- Mackas, D., Bohrer, R., 1976. Fluorescence analysis of zooplankton gut contents and an investigation of diel feeding patterns. *J. Exp. Mar. Biol. Ecol.* 25 (1), 77–85.
- Manno, C., Stowasser, G., Enderlein, P., Fielding, S., Tarling, G.A., 2015. The contribution of zooplankton faecal pellets to deep-carbon transport in the Scotia Sea (Southern Ocean). *Biogeosciences* 12, 1955–1965.
- Marty, J.C., Goux, M., Guigue, C., Leblond, N., Raimbault, P., 2009. Short-term changes in particulate fluxes measured by drifting sediment traps during end summer oligotrophic regime in the NW Mediterranean Sea. *Biogeosciences* 6, 887–899.
- McDonnell, A.M., 2011. Marine Particle Dynamics: Sinking Velocities, Size Distributions, Fluxes, and Microbial Degradation Rates (Ph.D. Thesis). Massachusetts Institute of Technology.
- McDonnell, A.M.P., Buesseler, K.O., 2012. A new method for the estimation of sinking particle fluxes from measurements of the particle size distribution, average sinking velocity, and carbon content. *Limnol. Oceanogr.: Methods* 10, 329–346.
- Møller, E.F., Borg, C.M.A., Jónasdóttir, S.H., Satapoomin, S., Jaspers, C., Nielsen, T.G., 2010. Production and fate of copepod fecal pellets across the Southern Indian Ocean.

- Mar. Biol. 158, 677–688.
- Neuer, S., Davenport, R., Freudenthal, T., Wefer, G., Llinás, O., Rueda, M.J., Steinberg, D.K., et al., 2002. Differences in the biological carbon pump at three subtropical ocean stations. *Geophys. Res. Lett.* 29 (32–31).
- Neuer, S., Torres-Padron, M.E., Gelado-Caballero, M.D., Rueda, M.J., Hernandez-Brito, J., Davenport, R., Wefer, G., 2004. Dust deposition pulses to the eastern subtropical North Atlantic gyre: does ocean's biogeochemistry respond? *Glob. Biogeochem. Cycles* 18 (4), GB4020.
- Nowald, N., Fischer, G., Ratmeyer, V., Iversen, M., Reuter, C., Wefer, G., 2009. In-situ sinking speed measurements of marine snow aggregates acquired with a settling chamber mounted to the Cherokee ROV. *Oceans 2009 -Eur.* 1–2, 1286–1291.
- O'Brien, K.R., Waite, A.M., Alexander, B.L., Perry, K.A., Neumann, L.E., 2006. Particle tracking in a salinity gradient: a method for measuring sinking rate of individual phytoplankton in the laboratory. *Limnol. Oceanogr.-Methods* 4, 329–335.
- Oguri, K., Matsumoto, E., Yamada, M., Saito, Y., Iseki, K., 2003. Sediment accumulation rates and budgets of depositing particles of the East China Sea. *Deep-Sea Res. Part II* 50, 513–528.
- Paffenhofer, G.A., Knowles, S.C., 1979. Ecological implications of fecal pellet size, production and consumption by copepods. *J. Mar. Res.* 37 (1), 35–49 (1).
- Pakhomov, E.A., Froneman, P.W., Wassmann, P., Ratkova, T., Arashkevich, E., 2002. Contribution of algal sinking and zooplankton grazing to downward flux in the Lazarev Sea (Southern Ocean) during the onset of phytoplankton bloom: a lagrangian study. *Mar. Ecol. Prog. Ser.* 233, 73–88.
- Passow, U., 2002. Transparent exopolymer particles (TEP) in aquatic environments. *Prog. Oceanogr.* 55, 287–333.
- Peinert, R., Saure, A., Stegmann, P., Stienen, C., Haardt, H., Smetacek, V., 1982. Dynamics of primary production and sedimentation in a coastal ecosystem. *Neth. J. Sea Res.* 16, 276–289.
- Peperzak, L., Colijn, F., Koeman, R., Gieskes, W.W.C., Joordens, J.C.A., 2003. Phytoplankton sinking rates in the Rhine region of freshwater influence. *J. Plankton Res.* 25, 365–383.
- Pesant, S., Legendre, L., Gosselin, M., Bauerfeind, E., Budéus, G., 2002. Wind-triggered events of phytoplankton downward flux in the Northeast Water Polynya. *J. Mar. Syst.* 31, 261–278.
- Pilskaln, C.H., Churchill, J.H., Mayer, L.M., 1998. Resuspension of sediment by bottom trawling in the Gulf of Maine and potential geochemical consequences. *Conserv. Biol.* 12, 1223–1229.
- Pitcher, G.C., Mitchell-Llnes, B.A., 1989. Phytoplankton sinking rate dynamics in the southern Benguela upwelling system. *Mar. Ecol. Prog. Ser.* 55 (2–3), 261–269.
- Ploug, H., Iversen, M.H., Koski, M., et al., 2008. Production, oxygen respiration rates, and sinking velocity of copepod fecal pellets: direct measurements of ballasting by opal and calcite. *Limnol. Oceanogr.* 53 (2), 469–476.
- Reynolds, C.S., 2006. *The Ecology of Phytoplankton* (Ph.D. Thesis). Cambridge University Press.
- Riemann, F., 1989. Gelatinous phytoplankton detritus aggregates on the Atlantic deep-sea bed. *Mar. Biol.* 100, 533–539.
- Roy, S., Silverberg, N., Romero, N., et al., 2000. Importance of mesozooplankton feeding for the downward flux of biogenic carbon in the Gulf of St. Lawrence (Canada). *Deep-Sea Res. Part 2* (47), 519–544.
- Sabine, C.L., Hood, M., 2003. Ocean carbon scientists organize to achieve better coordination, cooperation. *Eos Trans. Am. Geophys. Union* 84, 218.
- Sarno, D., Kooistra, W.H.C.F., Medlin, L.K., Percopo, I., Zingone, A., 2005. Diversity in the genus *Skeletonema* (Bacillariophyceae). II. An assessment of the taxonomy of *S. costatum* like species with the description of four new species. *J. Phycol.* 41, 151–176.
- Seebah, S., Fairfield, C., Ullrich, M.S., Passow, U., 2014. Aggregation and sedimentation of *Thalassiosira weissflogii* (diatom) in a warmer and more acidified future ocean. *PLoS One* 9, e112379.
- Shanks, A.L., Trent, J.D., 1980. Marine snow: sinking rates and potential role in vertical flux. *Deep Sea Res. Part A Oceanogr. Res. Pap.* 27, 137–143.
- Smayda, Theodore J., 1997. Harmful algal blooms: their ecophysiology and general relevance to phytoplankton blooms in the sea. *Limnol. Oceanogr.* 42 (5), 1137–1153.
- Smetacek, V., von Bröckel, K., Zeitzschel, B., Zenk, W., 1978. Sedimentation of particulate matter during a phytoplankton spring bloom in relation to the hydrographical regime. *Mar. Biol.* 47, 211–226.
- Smith, S.L., Henrichs, S.M., Rho, T., 2002. Stable C and N isotopic composition of sinking particles and zooplankton over the southeastern Bering Sea shelf. *Deep Sea Res. Part II: Top. Stud. Oceanogr.* 49, 6031–6050.
- Steinberg, D.K., Landry, M.R., 2017. Zooplankton and the ocean carbon cycle. *Annu. Rev. Mar. Sci.* 9, 413–444.
- Strickland, J.D., Parsons, T.R., 1972. *A practical handbook of seawater analysis*. Fish. Res. Board Can.
- Sun, J., Liu, D., 2003. Geometric models for calculating cell biovolume and surface area for phytoplankton. *J. Plankton Res.* 25, 1331–1346.
- Svensen, C., Morata, N., Reigstad, M., 2014. Increased degradation of copepod faecal pellets by co-acting dinoflagellates and *Centropages hamatus*. *Mar. Ecol. Prog. Ser.* 516, 61–70.
- Tang, D., Di, B., Wei, G., Ni, I.H., Oh, I.S., Wang, S., 2006. Spatial, seasonal and species variations of harmful algal blooms in the South Yellow Sea and East China Sea. *Hydrobiologia* 568, 245–253.
- Tang, Y.Z., Egerton, T.A., Kong, L., Marshall, H.G., 2008. Morphological variation and phylogenetic analysis of the dinoflagellate *Gymnodinium aureolum* from from a Tributary of Chesapeake Bay. *J. Eukaryot. Microbiol.* 55, 91–99.
- Turner, J.T., 2002. Zooplankton fecal pellets, marine snow and sinking phytoplankton blooms. *Aquat. Microb. Ecol.* 27, 57–102.
- Turner, J.T., 2015. Zooplankton fecal pellets, marine snow, phytodetritus and the ocean's biological pump. *Prog. Oceanogr.* 130, 205–248.
- Vaillancourt, R.D., Marra, J., Seki, M.P., Parsons, M.L., Bidigare, R.R., 2003. Impact of a cyclonic eddy on phytoplankton community structure and photosynthetic competency in the subtropical North Pacific Ocean. *Deep Sea Res. Part I: Oceanogr. Res. Pap.* 50, 829–847.
- Waite, A., Bienfang, P.K., Harrison, P.J., 1992a. Spring bloom sedimentation in a sub-arctic ecosystem. *Mar. Biol.* 114, 131–138.
- Waite, A.M., Thompson, P.A., Harrison, P.J., 1992b. Does energy control the sinking rates of marine diatoms? *Limnol. Oceanogr.* 37, 468–477.
- Waite, A.M., Safi, K.A., Hall, J.A., Nodder, S.D., 2000. Mass sedimentation of picoplankton embedded in organic aggregates. *Limnol. Oceanogr.* 45 (1), 87–97.
- Walsby, A.E., 1978. The properties and buoyancy-providing role of gas vacuoles in *Trichodesmium* Ehrenberg. *Eur. J. Phycol.* 13, 103–116.
- Wang, R., Conover, R.J., 1986. Dynamics of gut pigment in the copepod *Temora longicornis* and the determination of in situ grazing rates. *Limnol. Oceanogr.* 31, 867–877.
- Wang, R., Fan, C., 1997. Copepods feeding activities and its contribution to downwards vertical flux of carbon in the East China Sea. *Oceanol. Et. Limnol. Sin.* 6, 003.
- Wilson, S.E., Steinberg, D.K., Buesseler, K.O., 2008. Changes in fecal pellet characteristics with depth as indicators of zooplankton repackaging of particles in the mesopelagic zone of the subtropical and subarctic North Pacific Ocean. *Deep Sea Res. Part II: Top. Stud. Oceanogr.* 55, 1636–1647.
- Wilson, S.E., Ruhl, H.A., Smith, K.L., 2013. Zooplankton fecal pellet flux in the abyssal northeast Pacific: a 15 year time-series study. *Limnol. Oceanogr.* 58, 881–892.
- Yoon, W.D., Kim, S.K., Han, K.N., 2001. Morphology and sinking velocities of fecal pellets of copepod, molluscan, euphausiid, and salp taxa in the northeastern tropical Atlantic. *Mar. Biol.* 139, 923–928.
- Zhu, Z.Y., Zhang, J., Wu, Y., Lin, J., 2006. Bulk particulate organic carbon in the East China Sea: tidal influence and bottom transport. *Prog. Oceanogr.* 69, 37–60.
- Zwanzig, R., 1964. Hydrodynamic fluctuations and Stokes' law friction. *J. Res. Natl. Bur. Stand.* 68, 143–145.